Non-focal non-thermal electrical methods for cancer treatment

Quim Castellví Fernandez

TESI DOCTORAL UPF / 2017

Directors:

Dr. Antoni Ivorra Cano
Dr. Bart Bijnens

Department of Information and Communication Technologies
Universitat Pompeu Fabra

This work was carried out in the Department of Information and Communication Technologies (DTIC) at Universitat Pompeu Fabra (UPF), Barcelona, Spain.

Quim Castellví Fernandez was supported by the *Programa Nacional de Formación de Profesorado Universitario* (FPU12/04920) from the Spanish Ministry of Education.

This work was supported by the Spanish government through grants (AR00311-MICINN-TEC2010-11182-E, SAF2012-33636, RTICCC RD 12/0036/0031, TEC2010-17285, TEC2011-27133-C02 and TEC2014-52383-C3 (TEC2014-52383-C3-1-R, TEC2014-52383-C3-2-R and TEC 2014-52383-C3-3-R), by the European Commission through the Marie Curie International Reintegration Grant TAMIVIVE (256376) and by the Generalitat de Catalunya (2009 SGR 1356).

Als meus pares i a la meva germana.

Abstract

Most physical ablation modalities for cancer treatment are focal and are based on thermal damage. Despite their regular clinical use as an alternative to surgical resection, their thermal principle of operation entails risks regarding the preservation of neighboring vital structures, such as large vessels, critical ducts or nerves. In addition, being focal, their use is unpractical in cases where multiple nodules are present or tumors are difficult to reach with the applicators.

This thesis explores non-thermal electrical treatments which can be applied in a non-focal manner. Two treatments have been investigated: the first treatment, proposed by others a few years ago, is based on the permanent application of low magnitude alternating electric fields through surface electrodes. Here, this treatment has been *in vivo* studied to evaluate its efficacy as well as to discern whether it is non-thermally mediated. The second electrical treatment is based on the electroporation phenomenon and targets liver tumor nodules. Electroporation-based therapies employ brief high magnitude electric fields. These pulsed fields, alone or in combination with chemotherapeutic drugs, are able to kill cells by increasing their membrane permeability. Current electroporation-based therapies for internal tumors are local and are delivered through needle-shaped electrodes. Rather than using needle electrodes to treat liver tumors, here it is explored a novel treatment in which large plate electrodes are used to deliver the field across the whole liver in a non local fashion. The treatment aims at simultaneously destroying all tumors while preserving healthy tissue. Its efficacy is based on selectively enhancing the electric field over the tumors by infusing a solution with high electrical conductivity.

The proposed treatment for liver tumors requires a high performance generator which is not currently available. The work presented here includes the design of a new generator topology able to fulfill the requirements.

Resum

La majoria del mètodes físics d'ablació tumoral es basen en produir dany tèrmic de manera focalitzada. Tot i ser considerats una alternativa habitual a la resecció quirúrgica, el principi tèrmic de funcionament, comporta un risc per la preservació d'estructures vitals adjacents a la zona de tractament, tals com grans vasos o nervis. A més, el fet de ser focals, fa impracticable la seva aplicació en cas de múltiples nòduls o tumors de difícil accés.

Aquesta tesi explora tractaments elèctrics no basats en temperatura, capaços de ser aplicats de manera no focal. S'han investigat dos tractaments: El primer, proposat per altres fa pocs anys, està basat en aplicar permanentment camps elèctrics alterns de baixa magnitud a través d'elèctrodes superficials. Aquí, aquest tractament s'ha estudiat *in vivo* tant per avaluar la seva eficàcia com per discernir si aquesta resideix en la temperatura. El segon tractament es basa en el fenomen d'electroporació i persegueix el tractament de nòduls hepàtics. En els tractaments basats en electroporació, s'apliquen breus camps elèctrics de gran magnitud per tal de permeabilitzar la membrana cel·lular. Això permet la penetració d'agents quimioterapèutics o produeix directament la mort cel·lular. En lloc d'utilitzar, com és habitual, agulles per tal d'aplicar el tractament, aquí s'explora tractar tot el fetge de forma no localitzada, fent servir grans elèctrodes plans i paral·lels. Utilitzant solucions d'alta conductivitat elèctrica, es pretén magnificar selectivament el camp elèctric sobre els tumors, sent així capaços de destruir tots els tumors i alhora preservar el teixit sà.

El tractament proposat per els tumors hepàtics, requereix d'un equip generador actualment no disponible. El presentat treball inclou el disseny d'una nova topologia de generadors capaç de complir amb els requisits.

Contents

Abstract **v**

Resum **vii**

Acronyms and abbreviations **xiii**

1 Introduction **1**
1.1 State of the art and motivation 3
1.2 Research goal 8
1.3 Dissertation overview 8

2 Background **11**
2.1 Electric field effects on biological tissue 13
2.2 Alternating electric fields for cancer treatments 18
2.2.1 Operating principle 18
2.2.2 Treatment application 19
2.3 Electroporation for cancer treatments 21
2.3.1 Operating principle 21
2.3.2 Treatment application 23
2.4 Numerical modeling of electric fields distribution in tissue 25
2.4.1 Electric equivalent model for tissue 27

3 Tumor growth delay by adjuvant alternating electric fields **37**
3.1 Introduction 39
3.2 Materials and methods 41
3.2.1 Treatment devices 41
3.2.2 Simulation of the treatment setup 43

3.2.3 *In vivo* study 46
3.3 Results 48
3.3.1 Simulation of the treatment setup 48
3.3.2 Treatment results 49
3.4 Discussion 51
3.5 Conclusions 55
3.6 Appendix 55

4 Modular pulse generator for electroporation 59
4.1 Introduction 61
4.1.1 Pulse generator topology 61
4.1.2 IRE assessment in tissue 66
4.2 Materials and methods 67
4.2.1 Proposed modular concept 67
4.2.2 Implementation of the prototype 70
4.2.3 Assessment with vegetable model 71
4.3 Results 74
4.3.1 Electrical characterization of the prototype . . 74
4.3.2 Assessment with vegetable model 75
4.4 Conclusions 78

5 Selective transhepatic electroporation by means of hypersaline infusion 79
5.1 Introduction 81
5.2 Numerical study on treatment feasibility 84
5.2.1 Introduction 84
5.2.2 Materials and methods 84
5.2.3 Results 86
5.2.4 Discussion 88
5.2.5 Conclusions 89
5.3 Modeling liver electrical conductivity during hypertonic injection 89
5.3.1 Introduction 89
5.3.2 Materials and methods 90
5.3.3 Results 99
5.3.4 Discussion 102
5.3.5 Conclusions 104
5.3.6 Appendix 105
5.4 Irreversible electroporation of a large portion of the liver 109
5.4.1 Introduction 109
5.4.2 Materials and methods 110
5.4.3 Results 112

5.4.4 Discussion 114
5.5 Conclusions 116

6 Conclusions **119**
6.1 General conclusions 121
6.2 Future perspective 122

Bibliography **125**

List of publications **151**

Acronyms and abbreviations

ABS	Acrylonitrile butadiene styrene
ac	Altern current
CSF	Cerebrospinal fluid
dc	Direct current
DNA	Deoxyribonucleic acid
EChT	Electrochemical therapy
ECT	Electrochemotherapy
EMI	Electromagnetic interference
ESOPE	European standard operating procedure of electrochemotherapy
EU	Energy unit
FDA	Food and drug administration
FEM	Finite element method
GBM	Glioblastoma multiforme
H-FIRE	High-frequency irreversible electroporation
HIFU	High-intensity focused ultrasound
HS	Hypersaline solution
HV	High voltage
I^2C	Inter-integrated circuit
ICP-MS	Inductively coupled plasma mass spectrometry
IGBT	Insulated gate bipolar transistor
IHP	Isolated hepatic perfusion
i.p.	Intraperitoneal
IRE	Irreversible electroporation
i.v.	Intravenous
LV	Low voltage
MOSFET	Metal oxide semiconductor field effect transistor
MWA	Microwave ablation
nsPEF	Nanosecond pulsed electric fields
NTIRE	Non-thermal irreversible electroporation
OS	Overall survival
PBPK	Physiologically based pharmacokinetic
PCB	Printed circuit board

PDAC	Pancreatic ductal adenocarcinoma
PhD	Philosophiæ doctor
PMMA	Polymethyl methacrylate
PTC	Positive temperature coefficient
RBC	Red Blood Cell
RFA	Radiofrequency ablation
s.c.	Subcutaneous
SD	Standard deviation
SoC	System on a chip
STEP-HI	Selective transhepatic electroporation by means of hypersaline infusion
SU	Switching unit
TTFields	Tumor treatment fields
UPF	Universitat Pompeu Fabra

Chapter 1

Introduction

1.1 State of the art and motivation

Cancer is one of the main causes of death worldwide with more than 14 million of new cases diagnosed per year [1]. And the growth and aging of the population anticipate a rising trend in cancer cases [2].

In the battle against cancer, there are three categories of treatment considered as the standard armamentarium to eradicate cancer in a patient. Namely, surgical resection, radiotherapy and chemotherapy.

Surgical resection entails physical excision of the undesired tumor tissue. Currently, this approach is considered as the most effective for solid tumors [3]. Unfortunately, in order to get access and eradicate all possible malignant cells, surgical resection often involves the excision of a large volume of surrounding healthy tissue. In case of tumors located close to vital structures (e.g. brain, spinal cord or large blood vessels), surgical resection is not an option [4].

Radiation therapy is normally chosen when surgery is not feasible. This treatment modality relies on damaging the DNA molecules of cancer cells with high energy ionizing radiation (e.g. X-ray or protons). Ionizing radiation can damage the DNA of cancer cells and this commonly leads to cell division impairment. The radiation can be delivered from outside the patient's body by an external equipment that generates a radiation beam pointed to the target tissue (external beam radiation therapy). Radiation can also be delivered internally by using radioactive isotopes confined in capsules known as *radioactive seeds* (brachytherapy). Unfortunately, not only the cancer cells are damaged by radiation. The amount of radiation, dosage, is limited to minimize the risks of affecting healthy tissues. Among those risks it is worth noting infertility, pulmonary fibrosis and induction of secondary tumors. Dosage limitation compromises both the efficacy and the capability of applying multiple radiation treatments over a short period of time [5].

The third well established treatment category for cancer treatment is the chemotherapy. Although it is employed as a successful primary treatment in case of non-solid cancer types, such as leukemia and lymphoma [6], its efficacy on treating solid tumors is limited [7]. It is usually used as an adjuvant therapy to another primary treatment in order to maximize chances of success [8; 9]. This treatment modality consists in introducing systemically a chemotherapeutic agent with antiproliferative effects on cells. Since the human body needs to continually regenerate cells, the inhibition of these processes involves a

multitude of side effects like fatigue, immune system deficiency, nausea and vomiting or hair loss [10].

In most of patients with solid tumors, surgical resection is generally the first treatment recommendation [6]. In patients not suitable for surgery, radiotherapy and/or chemotherapy are applied. In a lot of cases this is not done for destroying the tumor but to reduce its size for a future surgical procedure.

Following surgical resection or radiation of solid tumors, chemotherapy is often applied intending to eradicate any remaining cancer cells and to deal with the risk of metastasis [11].

A better knowledge of cancer biology allows the development of new therapeutics. In the last few years several innovative modalities for the treatment of solid tumors have emerged.

In addition to the well established chemotherapy, other pharmacological therapies are currently being used. It is well known that some tumor cells (e.g. breast and prostate cancer) growth according to the hormone levels [12]. Hormonal therapy is based on blocking the production of hormones or interfering in its behavior in order to stop the tumor cells proliferation [13]. Another promising approaches, already approved for human use, is the immunotherapy. In contrast to the rest of cancer therapies which focus on cancer cells as the main target, this type of cancer treatment try to helps the patient's immune system to recognize and destroy cancer by itself [14]. Provably the most ambitious type of treatment currently under intensive research is the gene therapy. This therapy pursuits the correction of the malfunctioning genes in cancer cell by introducing a correct copy of those [15]. Despite the promising results shown by the new pharmacological therapies when targeting an specific cancer cells [16], these not show significant response as a non-specific technique [17], thus, restricting its applicability.

Although advances in cancer treatment have enabled successful remissions, cancer cure remains largely elusive. Yet, many patients are still considered unsuitable for resection and with non radiation or pharmacological response [18]. The large number of patients unsuitable to undergo surgical resection has led to an emerging usage of alternative surgery treatments to resection.

Tumor ablation is a technique that attempts to destroy a specific focal tumor by producing chemical, thermal or electrical damage in a local manner [19]. In addition to the eradication of all the malignant

cells within a defined target volume, the ablative technique can safely minimize the destruction of surrounding healthy tissue to about 1 cm margin [20]. The technique is generally applied by minimally invasive procedures using needle-shape applicators and guided by medical images. This fact allows its usage in locations where traditional surgical resection is not an option.

The currently available techniques for focal tumor ablation consist in affecting the undesired tissue in a local manner. This techniques can be clearly categorized in thermal and non-thermal according to its principle of action.

The thermal treatments relies on the generation of high temperatures ($> 50°C$ [21]) to induce permanent cellular damage due to protein coagulation [22]. The induced heat within the tissue is commonly generated by means of electromagnetic waves (e.g. radiofrequency, microwave or laser) or ultrasounds (HIFU). In opposition to the increase in temperature, tissue ablation can also be achieved by decreasing and holding tissue temperature at -20$°C$ for one minute (cryoablation)[23]. One of the major problems of the current temperature ablation methods is the difficulty of altering the temperature in areas with high blood perfusion, such as the ones close to large blood vessels where the induced temperature increase is dissipated by the heat sink effect of blood flow [24]. Furthermore, since high temperature ablation implies the destruction of the extracellular matrix, tumors near to vital structures (e.g. gallbladder, bile ducts, bowel) are barely treatable with these techniques as thermal damage in these structures can result in fatal outcomes [25].

In order to overcome the limitations of thermal ablations, non-thermal modalities can be alternatively used. This type of techniques generally uses chemical agents or non-ionizing energy which provoke a local cell damage not based on a temperature change.

Percutaneous chemical ablation was an extensively used technique which use a multi-side-hole needle to inject a cytotoxic chemical agent (i.e. ethanol or acetic acid) at the tumor location. With this technique, a safely necrosis can be achieved in small tumors but the local tumor progression rate and the variability of the ablation zone have end up provoking its replacement by other ablative treatments [19].

Photodynamic therapy is a technique presented at the beginning of the 20th Century [26] which consists in injecting a photosensitizer agent that reacts with a light source. When this drug is exposed to bright

light with a certain wavelength, it generates a redox reaction producing singlet oxygen which has cytotoxic effects [27]. A major limitation of this technique is that light cannot penetrate deep into tissues (approximately just 1 cm). This makes the technique unfeasible for large or deep-seated tumors [28], hence, restricting its application to the tissue surfaces.

Although the delivery of electric current is always accompanied by heat, there is a set of therapies based on the delivery of current whose principle of action is non-thermal.

The so-called electrochemical treatment (EChT) consists in delivering continuous current between two or more electrodes located near or in the tumor itself. The electrochemical reaction produced at the electrodes interface alters the pH to levels where the cells cannot survive [29]. It is an easy and low cost technique that allows treating deep tumors by means of percutaneous needle-shaped electrodes. As in the case of percutaneous chemical ablation, one of the main drawbacks of this technique is the difficulty to accurately predict the ablated volume, therefore, to ensure the correct treatment over the whole target tissue is not straightforward [30].

Electroporation is the phenomenon in which cell membrane permeability to ions and macromolecules is increased by exposing the cell to short high electric field pulses [31]. Such increase in permeability is, presumably, related to the formation of nano-scale defects or pores in the cell membrane [32], and depending on the field intensity and duration, permeabilization can be transient or permanent. Reversible electroporation is the transient permeabilization of the cell membrane which do not compromise the cell survival *per se*. It has been extensively used as a microbiology laboratory technique to introduce into the cell, molecules unable to penetrate in normal circumstances [33]. The use of this reversible phenomenon to deliver anticancer drugs within malignant cells began in the 90s, resulting in the technique coined electrochemotherapy (ECT) [34]. It was not until 2004 that irreversible electroporation (IRE) was proposed as a tissue ablation method [35] which lies in the permanent or temporal membrane electroporation process that causes cells to die. IRE disrupts the cellular homeostasis causing the death of the cancer cell without requiring any drug to be delivered. A remarkable advantage of electroporation techniques is that, unlike in thermal methods, the extracellular matrix remains functional and, therefore, these treatments can be safely applied close to vital structures, such as large blood vessels [36]. Al-

though electroporation-based cancer therapies remain in in what can be considered to be an early stage of development, it must be noted that electrochemotherapy is currently employed in the clinic routine as treatment of cutaneous and subcutaneous tumors [37].

Overall, focal ablation therapies bring the opportunity to treat locations where traditional surgery procedures cannot be applied while minimizing the destruction of surrounding healthy tissue. These treatments show the potential to enlarge the number of patients suitable for surgical intervention. Unfortunately, technology limitations in focal therapies results in the inability to treat large volumes of tissue. Multiple studies report a dramatical decrease in treatment success rates as the size of the tumor increases beyond 3 cm [38; 39; 40; 41; 42]. In addition, treatment success also seem to be related to the number of tumors showing the poorest outcome in patients with more than three nodules [43].

Although focal ablation techniques allow to treat critical locations using needle-shape applicators, the required penetration in organs such as brain or lungs, could imply severe consequences. In addition, focal methods require a precise location of the target tissue and an accurate positioning of the treatment applicators. In order to overcome these drawbacks, few years ago a new method coined as *tumor treating fields* (TTFields) [44] was proposed to treat cancer tumors or, at least, slow down their progression. According to the researchers that initially developed the method, it is possible to disrupt the normal mitosis process of the cells by the permanent application of an alternating low-intensity electric field (about 3 V/cm) at high frequency (about 150 kHz). The greatest advantage of this treatment method lies in the ability to treat tumors using non-invasive surface electrode externally placed around the treatment area. On the other hand, it must be noted that their clinical results only show a modest efficacy in comparison with chemotherapeutic therapies [45].

In the context of emergence of non-thermal electrical methods for cancer treatment and in response to the limitations of focal tissue ablation techniques using needle-shape electrodes, research in non-focal modalities is of great interest to support and provide a fully understanding and validation of these treatments. The assessment of upcoming technologies and the development of new treatments is highly relevant considering the impact of this disease on the society.

1.2 Research goal

The main objective of the current PhD thesis is to contribute to the development and evaluation of emerging non-thermal electrical methods for cancer treatment. Specifically, this dissertation is focused on therapies based on the so-called TTFields and on the electroporation phenomenon. In response to the limitations of focal ablation techniques, this thesis targets new treatment techniques able to simultaneously treat multiple tumors without addressing them individually.

1.3 Dissertation overview

This dissertation explores therapeutic methods based on the so-called TTFields and on the electroporation phenomenon. Both sets of methods are based on the application of electric fields over the target tissue without involving a significant increase in temperature.

Chapter 2 underlines the principal effects of electric fields on biological tissues, how they can be used for tissue ablation and how some can be numerically predicted.

Chapter 3 presents an *in vivo* study of TTFields treatments pursuing a better understanding of the mechanisms of action while performing an independent evaluation of the treatment effectiveness. The study is carried out under the hypothesis that positive outcomes reported are mainly due to a mild hyperthermia rather than the electric-based mechanism stated by the promoters of the technique.

Next, electroporation-based studies are introduced. In order to explore novel modalities of treatment using this technique, it is priorly required the development of new tools currently not available. Chapter 4 provides a description of the design and development of a modular pulse generator able to fulfill the requirements in a flexible manner. The presented generator has been tested both using synthetic loads and living tissue. With the aim of minimizing the unnecessary animal experimentation, an improved procedure to *in vivo* assess electroporation treatment is presented using vegetable models.

Subsequently, taking advantage of the enhanced capabilities and flexibility of the proposed generator, in Chapter 5 a novel electroporation technique is presented able to simultaneously treat multiple tumor nodules in the liver while sparing the healthy tissue. This technique is based on injecting high conductivity solutions within the liver. In this chapter, a numerical feasibility study is firstly provided. In order

to estimate the increase of liver conductivity by means of portal saline injection, a mathematical model is also described. This tool can be used to predict the distribution of hypertonic solutions within the organ and to estimate the resulting electrical conductivity. Finally *in vivo* data collected during the pilot study is presented and compared with the expected results.

Lastly, Chapter 6 overviews the major findings and highlights the future directions of this research.

Chapter 2

Background

Abstract — This chapter presents background information necessary to understand subsequent sections of the dissertation. It starts with a summary of the principal effects of electric fields on biological tissues. Following, the operating principle and applicability for cancer treatment of both TTFields and electroporation are described. Finally, as the target treatments depend on the electric field magnitude, the basic concepts required to understand the electric field distribution in biological tissues are presented. That knowledge also supports the performance of numerical simulations in oder to predict the treatment outcomes.

Part of the contents of this chapter is adapted from:

Q. Castellví, "Bioimpedance Measurements and the Electroporation Phenomenon," *Revue 3EI*, vol. 75, pp. 21–26, 2014.

Q. Castellví, B. Mercadal, and A. Ivorra, "Assessment of Electroporation by Electrical Impedance Methods," in *Handbook of Electroporation*, D. Miklavčič, Ed. Springer International Publishing, pp. 1–20, 2016.

Chapter 2 removed due to copyright issues

Chapter 3

Tumor growth delay by adjuvant alternating electric fields

Abstract — Delivery of the so-called TTFields (Tumor Treatment Fields) has been proposed as a cancer therapy. These are low magnitude alternating electric fields at frequencies from 100 to 300 kHz which are applied continuously in a non-invasive manner. Electric field delivery may produce an increase in temperature which cannot be neglected. We hypothesized that the reported results obtained by applying TTFields *in vivo* could be due to heat rather than to electrical forces as previously suggested. Here it is presented an *in vivo* study in which pancreatic tumors subcutaneously implanted in nude mice were treated for a week either with mild hyperthermia (41°C) or with TTFields (6 V/cm, 150 kHz) and tumor growth was assessed. Although the TTFields applied singly did not produce any significant effect, the combination with chemotherapy did show a delay in tumor growth in comparison to animals treated only with chemotherapy (median relative reduction = 47%). We conclude that concomitant chemotherapy and TTFields delivery show a beneficial impact on pancreatic tumor growth. Contrary to our hypothesis, this impact is non-related with the induced temperature increase.

Part of the contents of this chapter is adapted from:

Q. Castellví, M. M. Ginestà, G. Capellà, and A. Ivorra, "Tumor growth delay by adjuvant alternating electric fields which appears non-thermally mediated," *Bioelectrochemistry*, vol. 105, pp. 16–24, 2015.

Chapter 3 removed due to copyright issues

Chapter 4

Modular pulse generator for electroporation

Abstract — A different magnitude, shape and duration of electric pulses are required depending on the electroporation application. So far, a different pulse generators devices has been necessary for each type of application. In this chapter it is presented the design of a pulse generator able to cover both current and future electric pulse requirements. First, a short review of common employed topologies and commercial devices for electroporation pulse generation are discussed highlighting the current limitations. Secondly, the proposed generator topology based on a modular configurations is presented. Following, a proof-of-concept prototype implementation is described and the assessment results are presented using both resistive load and vegetable tissue. Complementary, this chapter presents a novel method for IRE assessment on potato tubers. Both the novel pulse generator device and the *in vivo* assessment method show the potential to become useful tools in the electroporation research field.

Part of the contents of this chapter is adapted from:

H. Sarnago, Ó. Lucía, A. Naval, J. M. Burdío, Q. Castellví, and A. Ivorra, "A Versatile Multilevel Converter Platform for Cancer Treatment Using Irreversible Electroporation," *IEEE J. Emerg. Sel. Top. Power Electron.*, vol. 4, no. 1, pp. 236–242, 2016.

C. Bernal, Ó. Lucía, H. Sarnago, J. M. Burdío, A. Ivorra, and Q. Castellví, "A review of pulse generation topologies for clinical electroporation," *IECON 2015 - 41st Annu. Conf. IEEE Ind. Electron. Soc.*, pp. 625–630, 2016.

Q. Castellví, J. Banús, and A. Ivorra, "3D Assessment of Irreversible Electroporation Treatments in Vegetal Models," in *1st World Congress on Electroporation and Pulsed Electric Fields in Biology, Medicine and Food & Environmental Technologies*, pp. 294–297, 2016.

Chapter 4 removed due to copyright issues

Chapter 5

Selective transhepatic electroporation by means of hypersaline infusion

Abstract — Metastases in the liver frequently grow as scattered tumor nodules which neither can be removed by surgical resection nor focally ablated. In this chapter, it is presented a novel electroporation treatment in which field delivery is not local. With this technique, all the tumor nodules will be selectively treated using large plate electrodes located at both sides of the liver. By infusing an hypersaline solution of high electrical conductivity through the portal vein, the conductivity of healthy tissues and tumor nodules will be made significantly different so that the electric field will be focused on the undesirable tissues. First, numerical simulations were used to evaluate the feasibility of the proposed technique. Aiming to assess the capability of increasing the global conductivity of the liver, here it is also presented a mathematical model developed to estimate the NaCl distribution within the liver and the resulting conductivity change. The model fuses well-established compartmental pharmacokinetic models of the organ with the saline injection models employed for resuscitation treatments and it considers changes in sinusoidal blood viscosity due to the hypertonicity of the solution. Both mathematical simulations and *in vivo* results show the feasibility of increasing four times the conductivity of the healthy liver, which is suitable for the further development of the technique. Moving forward in the technique development, an *in vivo* experiment in mice was carried out where a large portion of liver was treated by IRE. In these experiments we observe the sudden death of mice after the treatment. This chapter also prove the relationship between those deaths and the massive release of potassium from the destroyed cells. This finding could be crucial to avoid the future appearance of similar problems in clinical practice.

Part of the contents of this chapter is adapted from:

Q. Castellví, P. Sánchez-Velázquez, E. Berjano, F. Burdío, and A. Ivorra, "Selective Electroporation of Liver Tumor Nodules by Means of Hypersaline Infusion: A Feasibility Study," in *6th European Conference of the International Federation for Medical and Biological Engineering*, pp. 821–824, 2015.

Q. Castellví, P. Sánchez-Velázquez, X. Moll, E. Berjano, A. Andaluz, F. Burdío, B. Bijnens and A. Ivorra, "Modeling Liver Electrical Conductivity during Hypertonic Injection," *Int. j. numer. method. biomed. eng.*, pp. 1–23, 2017.

P. Sánchez-Velázquez, Q. Castellví, A. Villanueva, R. Quesada, C. Pañella, M. Cáceres, D. Dorcaratto, A. Andaluz, X. Moll, M. Trujillo, J. M. Burdío, E. Berjano, L. Grande, A. Ivorra, F. Burdío, "Irreversible electroporation of the liver: is there a safe limit to the ablation volume?," *Sci. Rep.*, vol. 6, p. 23781, 2016.

5.1 Introduction

The liver has a distinctive blood supply in which blood comes from two different pathways. About 70% of blood comes from the portal vein whereas the remaining supply comes from the hepatic artery [173]. Both afferent vessels branch into venules and arterioles, eventually draining into the sinusoids, which are capillaries with fenestrations along their endothelial wall. These fenestrations allow the passage of small particles from the sinusoids to the hepatocytes across the interstitial space that surrounds the hepatocytes (Figure 5.1). Blood leaves the liver lobules through the central vein and it finally drains into the cava vein [174].

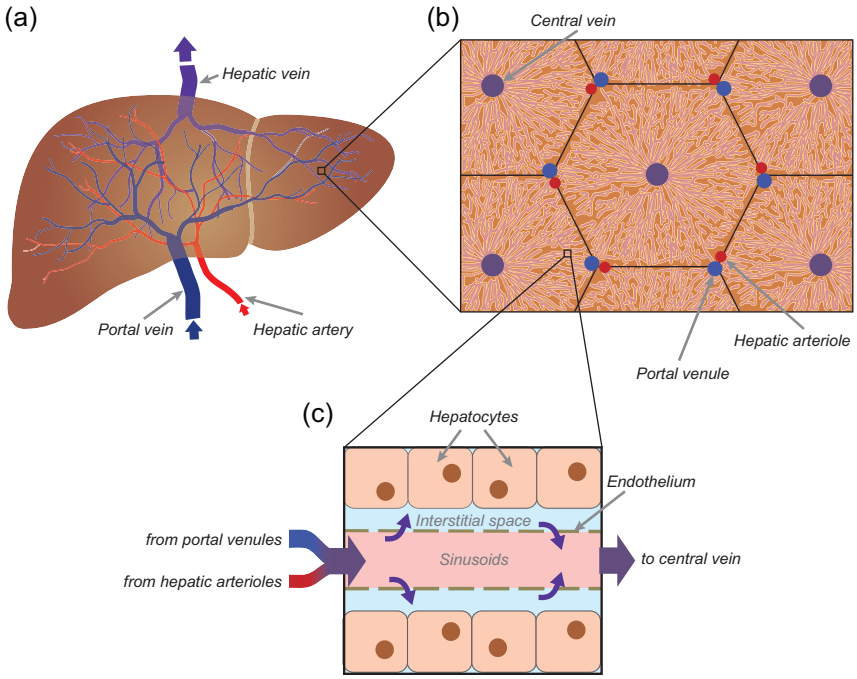

Figure 5.1: Schematic representation of liver anatomy: (a) At organ level. (b) Hepatic lobule level. (c) Sinusoidal microcirculatory level.

The dual blood supply of the liver and the presence of fenestrations in the sinusoids increase the likelihood of metastatic deposits in the liver [175]. Almost any primary cancer can spread to the liver commonly growing as scattered nodules [176] (Figure 5.2). About half of the patients with colorectal cancer develop hepatic metastases and less than 30% of those patients are suitable for surgical resection [177]. Either because tumors are adjacent to principal blood vessels or the removal

of healthy tissue associated with collateral damage from surgery would be too large for the patient's survival [178], entailing a poor prognosis for those patients.

Figure 5.2: Transversal section at liver with multiple tumor nodules. Healthy tissue enhancement by contrast introduced through portal vein [179].

In addition to surgical resection, the current medical armamentarium includes a set of loco regional therapies for ablating malignant liver tissues which can be applied to patients who are non-surgical candidates because of comorbidity or extensive disease. These focal liver ablation techniques include percutaneous ethanol injection, radiofrequency ablation, high-intensity focused ultrasound, microwave ablation and cryosurgery [180]. These techniques, however, because of their focal nature, are not adequate for patients in which the number of scattered nodules is large (> 3) [181].

Since electroporation does not involve thermal or chemical damage to the extracellular matrix, it allows to retain the structural integrity of the blood vessels and the nerves [182]. This fact allows treatment of tumors located close to critical structures which are unsuitable to be treated with other focal ablation techniques based on high-temperature. However, while IRE shows promising results treating non-resectable tumors [183], as a focal therapy, it is only recommended for treatment of less than three nodules with relatively small dimensions (< 5 cm) [181].

Interestingly, while healthy hepatocytes receive both arterial and venous blood, tumor nodules have a disorganized vascular structure, lacking sinusoids, which implies they are almost only supplied with arterial blood coming from the hepatic artery [184]. This fact is cur-

rently used for identifying tumors by the injection of contrast agents during medical imaging (Figure 5.2). Radiologists introduce the contrast solution by arterial infusion. Approximately 30 seconds after infusion the solution reaches the liver via portal vein (portal phase). Tumor nodules appear in the image as dark areas since the highlighting only affects at the healthy liver tissue.

Taking advantage of this fact, and inspired by previous studies on the use of conductive fluids to modulate the electric field during electroporation [120; 121], Dr. Fernando Burdío, from the Hospital del Mar (Barcelona, Spain), proposed to infuse hypersaline solution – i.e. with high electrical conductivity – through the portal vein for selectively electroporating tumor nodules when the electric field is applied through the whole liver parenchyma. The hypersaline solution would cause an increase in the conductivity of the healthy tissue whereas the conductivity in the tumor nodules is kept constant, so that, when potential difference is applied between opposite sides of the liver, the electric field magnitude in the tumors would be significantly larger than in the rest of the tissue.

In this way, it would be possible to cause electroporation of the tumor nodules while avoiding the effect in healthy parenchyma. This approach would have some major advantages with respect to the focal ablation techniques used in non-resectable tumor nodules. Namely, it would not be required to identify the exact position of the tumor nodules during the intervention and it would be possible to treat several tumor nodules at the same time making unnecessary to address them individually.

This novel electroporation technique has been proposed and developed by a multidisciplinary team comprising surgeons, physiologists, veterinarians, biologists and engineers. Supported by the Spanish Ministry, the global objective of the project was to explore the capabilities of electrical treatments to push beyond the current therapeutic techniques.

In this chapter it is presented the different studies performed in order to evaluate the feasibility of this novel technique and for its further development towards the clinical implementation.

5.2 Numerical study on treatment feasibility

5.2.1 Introduction

The first study carried out after the technique conceptualization, aimed to asses the feasibility of the proposed technique and to define its requirements, capabilities and limitations. This section presents a simplified numerical study using synthetic geometries and parameters extracted from the literature. As no data were available regarding the capabilities of hypertonic solutions to globally increase the electrical conductivity of the liver, a wide range of enhanced liver conductivities were studied.

5.2.2 Materials and methods

Numerical simulations were carried out with a geometrical model (Figure 5.3) which represents a cylindrical portion of liver (15 mm radius and 30 mm height) in which three tumor nodules are represented as spheres (radius 3 mm). High voltage was applied between parallel plates located at the top and bottom of the liver.

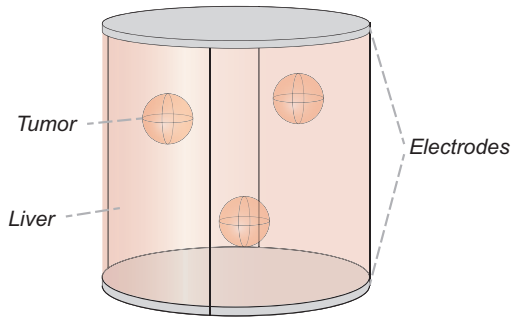

Figure 5.3: Geometrical model used in the numerical study. The model included three different elements: metallic electrodes, hepatic tissue, and tumor tissue.

The top interface between electrode was set to an electric potential ($\varphi = U$) while the bottom interface was set to ground ($\varphi = 0$). The electric field ($-\nabla\varphi$ or E) distribution within the three-dimensional geometry was obtained by solving the electric potential that satisfies:

$$\nabla \cdot (\sigma(|E|)\nabla\varphi) = 0 \tag{5.1}$$

where φ represents the electric potential and σ represent material conductivity. Notice that the electrical conductivity of the material

in equation 5.1 is not defined as a constant but a function dependent on electric field magnitude. When electroporation occurs, cell membrane conductivity increases, thus low frequency current will be able to flow through the cell. Therefore, for the relatively long pulses of electroporation (around 100 μs), the electrical conductivity of the tissue shows a dependence on the electric field magnitude ($|E|$). Several studies have pointed out that in order to correctly assess the electric field distribution within an biological tissue during electroporation treatments, it is important to use a non-linear model of the tissue conductivity [107]. Here, a sigmoid dependency between specific conductivity and electric field intensity is used [110]:

$$\sigma(|E|) = \sigma_0 + \frac{\Delta\sigma}{1 + 10e^{-\frac{|E|-A}{B}}} \tag{5.2}$$

$$A = \frac{E_{rev} + E_{ire}}{2} \tag{5.3}$$

$$B = \frac{E_{ire} - E_{rev}}{8} \tag{5.4}$$

where σ_0 denotes the non-electroporated conductivity, $\Delta\sigma$ represents the maximum increase in conductivity during the pulse, attributed to a fully permeabilized tissue, and where parameters A and B depend on the reversible (E_{rev}) and irreversible (E_{ire}) electric field thresholds. The parameter values employed for liver and tumor tissue are summarized in Table 5.1.

Table 5.1: Properties of the materials used in the theoretical model.

Material	σ_0 (S/m)	$\Delta\sigma$ (S/m)	E_{rev} (V/cm)	E_{ire} (V/cm)	References
Liver	0.126	0.335	460	700	[185; 110]
Tumor	0.269	0.254	460	700	[185; 110]

It can be expected that the injected saline mixes with the extracellular medium of the healthy liver, thus, raising the basal conductivity (σ_0). In order to study the outcomes at different level of conductivity increase due to hypersaline, a set of basal conductivities were employed ranging from 1 to 10 the normal basal conductivity (0.126 (S/m)). Figure 5.4 shows the employed conductivity functions for tumor, normal liver and an example of liver with a four times increased conductivity due to the injected hypersaline solution.

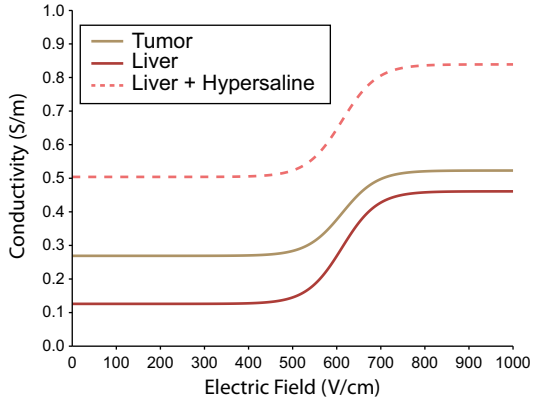

Figure 5.4: Representation of the non-linear functions employed to model the electrical conductivity as function of applied electric field for tumor, liver and liver with hypersaline.

Numerical simulations of irreversible electroporation treatment were performed. The relative amounts of treated tumor volume and also of the treated healthy tissue were assessed applying a voltage between the electrodes from 0 to 2500 V in steps of 5 V. Treatment was consider effective when the electric field magnitude surpassed the threshold of irreversible electroporation for a protocol of 8 pulses of 100 μs (700 V/cm [110]).

Specific finite element methods (FEM) simulation software (COMSOL Multiphysics, v.4.3, COMSOL Inc.) was used to numerically solve the described equations on the defined geometry and with the defined boundary conditions.

5.2.3 Results

Depending on electric potential applied between electrodes, the electric field generated within the tissue will cause the irreversible electroporation effect at certain tissue volume. Figure 5.5 shows the relative volume fraction of tumor and liver tissue affected by electroporation according to voltage applied between electrodes.

In case of normal conductivity of liver – i.e. without hypersaline injection – (Figure 5.5(a)), the sufficient voltage to produce irreversible electroporation of the whole ($> 99.9\%$) tumor tissue is 2170 V, also would suppose the overtreatment of the whole healthy tissue. The electric field distribution within the liver in this case can be observed in Figure 5.6(a).

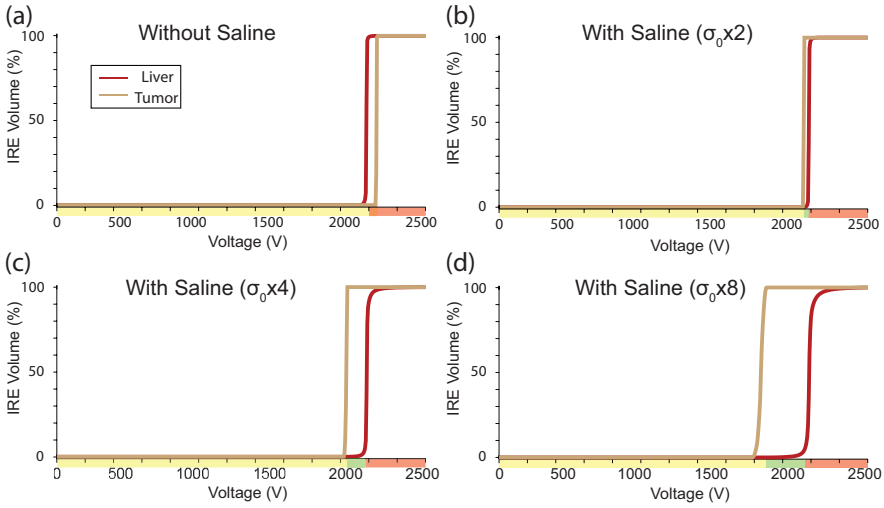

Figure 5.5: Relative volume of tissue irreversibly treated by electroporation in relation to the voltage applied between electrodes: (a) without hypersaline infusion ($\sigma_0 \times 1$). (b) with hypersaline ($\sigma_0 \times 2$). (c) with hypersaline ($\sigma_0 \times 4$). (d) with hypersaline ($\sigma_0 \times 8$).

On the other hand, Figure 5.5 (b-d) shows the relative volume ablation in cases where hypertonic saline solution is used, assuming an increase of liver conductivity 2, 4 and 8 times the normal liver conductivity (σ_0). In these cases, the minimum voltage required for the tumor treatment (2065 V, 1965 V and 1810 V respectively) generates electric field magnitudes within the healthy liver (Figure 5.6 (b-d)) that do not suppose an irreversible damage.

The maximum treatment magnitude which preserve the healthy liver ($< 5\%$ of damage) depends on the conductivity increase factor. Figure 5.6 (e-h) show the electric field distribution at this maximum treatment magnitude (2090 V, 2095 V, 2085 V and 2070 V) depending on the conductivity increase factor (1, 2, 4 and 8 respectively).

For each of the studied cases (conductivity increase ratio from 1 to 10) three main ranges of voltage can be defined according to the outcomes: Low voltage magnitudes do not induce enough electric field in the tumor tissue meaning that not the whole tumor nodule will be ablated. Otherwise, for very high magnitudes the electric field generated at liver tissue overpass the irreversible threshold entailing the destruction of the whole healthy parenchyma. However, for an specific range of "optimal voltages" all the tumor tissue is ablated ($> 99.9\%$) while the healthy liver is not irreversibly damaged ($< 5\%$). As can be

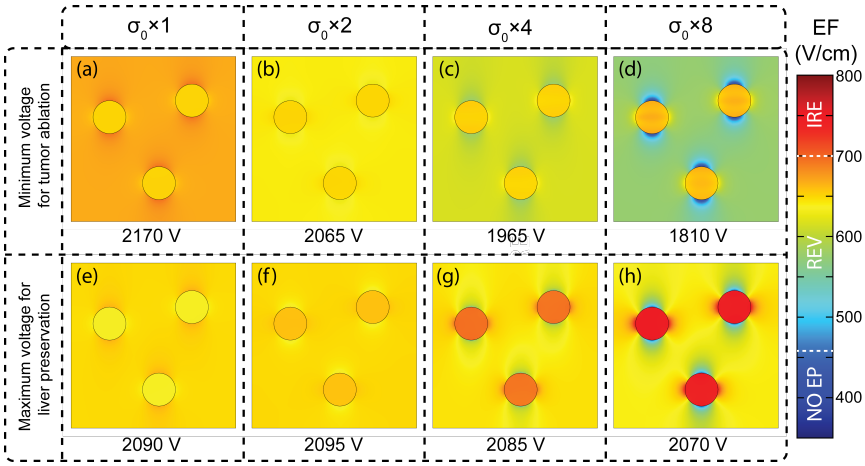

Figure 5.6: Electric field distribution within the tissue applying the minimum voltage for the whole (> 99.9%) tumor tissue. (a) Without saline ($\sigma_0 \times 1$) applying 2170 V between electrodes. (b) With saline solution ($\sigma_0 \times 2$) applying 2065 V between electrodes. (c) With saline solution ($\sigma_0 \times 4$) applying 1965 V between electrodes. (d) With saline solution ($\sigma_0 \times 8$) applying 1810 V between electrodes.

observed in Figure 5.5, the more increase in liver conductivity, the more distance between tumor and liver ablation exists. Figure 5.7 show the magnitude of this range as function of increased conductivity factor.

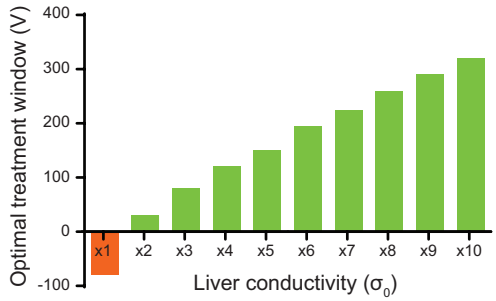

Figure 5.7: Optimal treatment intensity window according to the increase on liver conductivity.

5.2.4 Discussion

In case of normal conductivity of liver – i.e. without hypersaline injection – (Figure 5.5(a)), the sufficient voltage to produce irreversible electroporation of the whole (> 99.9%) tumor tissue is 2170 V, also

would suppose the overtreatment of the whole healthy tissue. The electric field distribution within the liver in this case can be observed in Figure 5.6(a).

The simulated results show that exists a certain range of treatment intensity that affects the whole tumor tissue but not healthy one. The higher is the electrical conductivity of healthy tissue, the greater the voltage drop in the lower conductivity tumor. Therefore, the complete ablation of the tumor can be achieved with less applied voltage, widening the optimal range of treatment intensity as can be observed in Figure 5.7.

5.2.5 Conclusions

This section presents the first step towards the development of a new therapeutic approach able to broaden the use of electroporation therapies for treating hepatic tumors. Despite of being a high invasive treatment, against the trend towards minimally invasive approaches, this technique could offer a new opportunity for currently untreatable cases were multiple tumor nodules are present. The results presented in this study indicate that by means of hypersaline solution infusion it may be possible to produce selective electroporation focused on tumor tissue.

5.3 Modeling liver electrical conductivity during hypertonic injection

5.3.1 Introduction

Once studied the outcome dependence on liver conductivity, the second study presented here aims to assess the capabilities of hypersaline solution (HS) to globally increase the electrical conductivity of the liver. In order to elucidate the expected behavior of conductivity during the procedure, it is presented a comprehensive mathematical model developed to predict both the temporal distribution of solute within the liver and the resulting electrical conductivity of the tissue.

Several studies have performed mathematical models of the liver to computationally assess the pharmacokinetic behavior of a defined drug or chemical agent [186; 187; 188; 189]. These studies usually employed the so called physiologically based pharmacokinetic (PBPK) models which represent the anatomical and physiological structure of the organ by using interconnected fluidic compartments. However, as

the employed drug concentrations are commonly low, these models neglected osmotic effects which are relevant in our case. On the other hand, hypertonic saline infusions have been used in fluid resuscitation for hemorrhagic patients [190] and some mathematical models have been developed aiming to determine the distribution at systemic level [191]. Here we fuse both modeling approaches in a novel model using the transport functions employed in the PBPK models in combination with the osmotic formulation from resuscitation models.

To the best of our knowledge, no data exist on the use of conductive fluids for managing the global conductivity of the liver. Therefore, this study also includes a pilot experimental study conducted on Landrace pigs which validates the mathematical model and the viability of the technique.

5.3.2 Materials and methods

Liver conductivity

The electrical conductivity of a tissue at low frequency mainly depends on the extracellular solution conductivity and the structural morphology [192]. Among the chemical species that constitute the extracellular body fluids, sodium and chloride are the main contributors to the electrical conductivity, consequently, here it was assumed that only sodium and chloride ions contribute to the conductivity of the extracellular plasma [193].

By injecting a hypertonic NaCl solution into the bloodstream, the NaCl concentration of the plasma is altered. To determine the conductivity of plasma (σ_p) at different NaCl concentrations (C_p), experimental data reported on NaCl solutions [194] was fitted with an exponential function ($R^2 > 0.99$).

$$\sigma_p = 30.22 \, \frac{S}{m} \left(1 - e^{\frac{-C_p}{3135 \, \frac{mol}{m^3}}} \right) 1.02^{(T-20°C)} \tag{5.5}$$

The reported experimental data were obtained at 20°C, therefore, an additional term was added for being able to assess the conductivity at body temperature ($T = 37°C$) taking into account the exponential conductivity grow of 2°C experienced by ionic solutions [48].

Physiological blood conductivity (about 0.65 S/m) differs substantially from that of the plasma (about 1.57 S/m). This difference is

caused by the presence of red blood cells (RBCs) which, at low frequencies, can be considered as non-conductive elements [195]. Archie's law [196] is extensively used in geology to assess the equivalent electric conductivity of composite materials [197]. Similarly, Archie's law has also been employed to determine the electrical conductivity of biological tissues [195]. For a material composed by an aqueous medium with conductivity σ_{solv} and non-conductive particles occupying a volume fraction (ϕ_p), the effective conductivity of the material (σ_{eff}) can be expressed as:

$$\sigma_{eff} = \sigma_{solv}(1 - \phi_p)^m \tag{5.6}$$

where m is a factor dependent on the shape of particles. The blood is mainly a suspension of non conductive RBCs in solvent (plasma). Therefore, according to (equation 5.6), the electrical conductivity of blood in sinusoids (σ_s) depends on its plasma conductivity ($\sigma_{p,s}$) and the hematocrit value (h_s). According to the shape of erythrocytes, a value $m = 1.46$ has been reported [195], and thus:

$$\sigma_s = \sigma_{p,s}(1 - h_s)^{1.46} \tag{5.7}$$

The same method can be employed to compute the conductivity of the whole liver parenchyma. Using equation 5.6 for the specific case of the liver parenchyma, the clusters of hepatic cells can be considered as the non-conductive particles which occupy a certain volume ($V_{c,hp}$) of the parenchyma volume (V_P). According to the cluster shape, the conductivity of the liver can be approximated using a shape factor value (m) of 1.67 [195]:

$$\sigma_L = \sigma_{si}(1 - \frac{V_{c,hp}}{V_P})^{1.67} \tag{5.8}$$

In this case the solvent conductivity (σ_{si}) is assumed to be a mixture between the conductivities of blood at sinusoids (σ_s) and the plasma at the interstitium ($\sigma_{p,hp}$). For a material composed by n compounds with a specific electrical conductivity (σ_j) and volume fraction (ϕ_j), and randomly oriented – which is the case of the parenchyma [198] – the effective conductivity can be expressed as [197]:

$$\sigma_{eff} = \prod_{n=1}^{n} \sigma_j^{\phi_j} \tag{5.9}$$

Using equation 5.9 it is possible to compute the effective conductivity of the composite material consisting of the sinusoids and the interstitial liquid according with their respective volumes (V_s and $V_{p,hp}$):

$$\sigma_{si} = \sigma_s^{\frac{V_s}{V_s+V_{p,hp}}} \sigma_{p,hp}^{\frac{V_{p,hp}}{V_s+V_{p,hp}}} \tag{5.10}$$

Compartmental model

A mathematical model was developed aiming at assessing both the fluid and solute movement within the liver. This model provides the parameters required to estimate the electrical conductivity of the liver parenchyma according to the formulation previously described.

Based on already reported models [186; 187; 199], a compartment model was implemented (see Figure 5.8). The model has four macroscopic compartments. Two of them represent the intrahepatic portal and arterial vasculature and the other two represent the hepatic parenchyma which consists of sinusoids and hepatocellular plates.

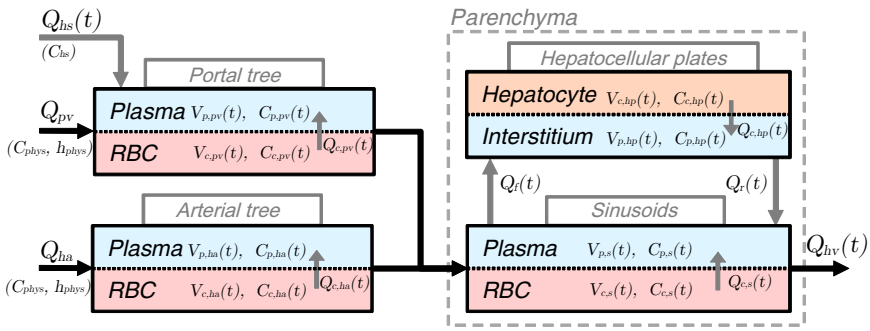

Figure 5.8: Representation of the compartmental model employed to simulate NaCl concentration. Composed by 8 sub-compartments, each one of them characterized by a volume V_x,y and an equivalent NaCl concentration $C_{x,y}$ where x denotes the extracellular (p) or intracellular (c) liquid and y denotes the macroscopic compartment (pv: Portal Vein, ha: Hepatic Artery, s: Sinusoids or hp: Hepatocellular Plates). Black arrows represent blood flow (movement of plasma liquid and RBC) while grey arrows symbolize liquid flow.

The model describes three supplying flows: one of these symbolizes the hypersaline infusion and the other two represent the normal incoming blood flows. The hypersaline solution flow (Q_{hs}), directly contributing to extracellular liquid in the portal vasculature, is modeled

as a square pulse with a magnitude according to the flow employed during the experiments and with the corresponding constant concentration (C_{hs}). Moreover, the blood supplies are characterized by their constant physiological flows (Q_{pv} and Q_{ha}), concentration (C_{phys}) and hematocrit (h_{phys}). Eventually blood exits from the sinusoids through the hepatic vein ($Q_{hv} = Q_{hs} + Q_{pv} + Q_{ha}$).

In the sinusoidal macroscopic compartment, plasma with concentration $C_{p,s}$, crosses, through the capillary wall, into the interstitial space in the hepatocellular plates at filtration flow rate Q_f and, at Q_r flow rate, interstitial fluid with concentration $C_{p,hp}$ is reabsorbed by the sinusoids.

The filtration and reabsorption flows (Q_f and Q_r) between the sinusoids and the interstitial space of the hepatocellular plates are commonly included in models as constant parameters. Here, in contrast, are considered to be pressure dependent. It is well known that filtration flow in sinusoids is determined by the capillary filtration coefficient (K_f) multiplied by the hydrostatic pressure difference between capillary and interstitium [200]. At the beginning of the sinusoid, closer form portal tract, sinusoidal pressure (P_s) is higher than the interstitial one (P_i) producing a filtration flow from the sinusoid to the interstitium.

$$Q_f(t) = K_f(P_s(t) - P_i(t)) \tag{5.11}$$

Moreover, closer to the hepatic vein, the capillary pressure (P_{hv}) is lower than interstitial producing the reabsorption flow.

$$Q_r(t) = K_f(P_i(t) - P_{hv}) \tag{5.12}$$

According to equations 5.11, 5.12 and the mass conservation, the filtration flow must be the same than the reabsorption flow, and this results in:

$$Q_f(t) = Q_r(t) = K_f(P_s(t) - P_{hv}) \tag{5.13}$$

For a defined capillary geometry and a constant blood flow, the resulting pressure at the entrance of the capillaries depends proportionally on fluid viscosity [201]. It has been reported a rapidly increase of pressure on microvascular structures once HS is injected into the blood

stream [202]. This increase of pressure is attributed to the HS effect on RBCs [203].

It has been also reported a dynamic viscosity almost linearly dependent with osmolarity [204]. Linearizing this reported data ($R^2 > 0.99$) at shear rate stress similar to the sinusoidal one (230 s^{-1}) blood viscosity can be expressed as function of cellular NaCl concentration ($C_{c,s}$) as:

$$\mu(t) = 4.59 \times 10^{-5} \frac{N \cdot m \cdot s}{mol} C_{c,s}(t) - 3.49 \times 10^{-3} \frac{N \cdots}{m^2} \tag{5.14}$$

Although the increase of viscosity affects the whole liver vasculature, the apparent viscosity in large vasculature (i.e. hepatic artery, portal vein and hepatic veins) does not increase as much as in the sinusoids [204]. Therefore, here it is only considered the viscosity dependence effect over the sinusoids.

This pressure can be estimated according to the hepatic vein vasculature pressure ($P_{hv,phys}$), the sinusoidal flow resistance ($R_{s,phys}$) and the viscosity (μ_{phys}) at physiological state, and along with the current blood flow through sinusoids ($Q_s = Q_{hv} - Q_r$) and the instantaneous blood viscosity (μ).

$$R_{s,phys} = \frac{P_{s,phys} - P_{hv,phys}}{Q_{s,phys}} \tag{5.15}$$

$$P_s(t) = P_{hv,phys} + Q_s(t) R_{s,phys} \frac{\mu(t)}{\mu_{phys}} \tag{5.16}$$

The amount of solute used in pharmacological studies is usually low. Therefore, the commonly employed PBPK models of the liver do not consider osmotic flow between compartments. However, as the HS osmolarity highly differs from the physiological one, the osmotic equilibrium plays an important role in the case modeled here. Thus, each one of the macroscopic compartments is divided into two subcompartments, one of them representing the extracellular liquid and the other representing the liquid confined within the cells. A difference in osmolarity between plasma and cellular sub-compartments leads to the water movement across the cell membrane (Q_c) trying to reach equilibrium. According to mathematical models used in the resuscitation field [191], the flow of water from cells to plasma (Q_c) depends on its membrane hydraulic conductivity (L_c), the cells plasma

surface area (S_c) – considered as constant – and the osmotic pressure difference between both compartments ($\Delta\Pi$).

$$Q_c(t) = L_c S_c \Delta\Pi \tag{5.17}$$

Although the ions within the cell differ from those found in the extracellular space, the osmolarity of both compartments is kept at the same value (308 mol/m^3). Therefore, for the sake of simplicity, as no exchange of solutes is assumed across the cell membrane, here the intracellular concentration is defined as a NaCl concentration although, in reality, the intracellular content differs from a NaCl solution. In other words, C_c indicates the concentration of NaCl that would produce the same osmolarity within the cell. C_c does not represent the actual concentration of intracellular species but it is proportional to it. Such simplification is just used for computing the osmotic pressure.

$$\Delta\Pi = RT(2C_p - 2C_c) \tag{5.18}$$

The osmotic pressure difference ($\Delta\Pi$) between two compartments is defined in equation 5.18 by their osmolarity (two times the concentration in case of a NaCl solution), the temperature ($T = 310$ K) and the gas constant ($R = 0.06236$ m^3·mmHg/(K·mol)).

The model computes the time course of the concentration in each sub-compartment. The liquid and solute exchanges are formalized by the physiological parameters shown in Table 5.2 and by the following differential equations derived from the conservation of mass. Runge-Kutta method was employed (MATLAB R2014b, The MathWorks Inc.) to solve the resulting system of equations:

$$\begin{aligned} V_{p,pv}(t)\frac{dC_{p,pv}(t)}{dt} &= C_{hs}Q_{hs}(t) + C_{phys}Q_{pv}(1 - h_{phys}) \\ &\quad - C_{p,pv}(t)\left((Q_{hs}(t) + Q_{pv})(1 - h_{pv}(t)) + Q_{c,pv}(t)\right) \end{aligned} \tag{5.19}$$

hi

$$\begin{aligned} V_{c,pv}(t)\frac{dC_{c,pv}(t)}{dt} &= C_{phys}Q_{pv}h_{phys} \\ &\quad - C_{c,pv}(t)\left((Q_{hs}(t) + Q_{pv})h_{pv}(t) - Q_{c,pv}(t)\right) \end{aligned} \tag{5.20}$$

Table 5.2: Physiological parameters employed in the model.

Symbol	Description	Value	Source
C_{phys}	Physiological NaCl concentration	154 mol/m^3	[191]
Q_{pv}	Flux of blood through portal vein	24.0 $ml/(min{\cdot}kg)$	[205]
Q_{ha}	Flux of blood through hepatic artery	8.4 $ml/(min{\cdot}kg)$	[205]
K_f	Filtration coefficient of sinusoids	3 $ml/(min{\cdot}mmHg{\cdot}kg)$	[200]
$P_{s,phys}$	Physiological pressure at sinusoids	4.4 $mmHg$	[206]
$P_{hv,phys}$	Phys. pressure at the hepatic vein	1.5 $mmHg$	[206]
h_{phys}	Physiological hematocrit	45%	[207]
V_L	Liver volume	30.3 ml/kg	[205]
V_{pv}	Portal vasculature volume	$13.3 \times 10^{-2}\, V_L$	See Appendix
V_{ha}	Hepatic artery vasculature volume	$4.6 \times 10^{-2}\, V_L$	See Appendix
$V_h v$	Hepatic vein vasculature volume	$16.2 \times 10^{-2}\, V_L$	See Appendix
V_P	Parenchyma volume	$65.9 \times 10^{-2}\, V_L$	V_L-V_{pv}-V_{ha}-V_{hv}
$V_(c, hp)$	Physiological hepatocyte volume	$77.8 \times 10^{-2}\, V_P$	[208]
$V_(p, hp)$	Physiological interstitial volume	$4.9 \times 10^{-2}\, V_P$	[208]
V_s	Sinusoidal volume	$10.6 \times 10^{-2}\, V_P$	[208]
ρ_L	Liver density	1070 kg/m^3	[209]
$S_{c,pv}$	RBC surface in portal vasculature	859.5 $cm^2/ml\ V_L$	[191] $h_{phys}\, V_{pv}$
$L_{c,pv}$	Membrane hydraulic conductivity	7.2×10^{-7} $ml/(min{\cdot}mmHg{\cdot}cm^2)$	[191]
$S_{c,ha}$	RBC surface in arterial vasculature	297.3 $cm^2/ml\ V_L$	[191] $h_{phys}\, V_{ha}$
$L_{c,ha}$	Membrane hydraulic conductivity	7.2×10^{-7} $ml/(min{\cdot}mmHg{\cdot}cm^2)$	[191]
$S_{c,s}$	RBC surface in sinusoids	451.5 $cm^2/ml\ V_L$	[191] $h_{phys}\, V_s$
$L_{c,s}$	Membrane hydraulic conductivity	7.2×10^{-7} $ml/(min{\cdot}mmHg{\cdot}cm^2)$	[191]
$S_{c,hp}$	Hepatocyte-interstitium surface	337.9 $cm^2/ml\ V_L$	See Appendix
$L_{c,hp}$	Membrane hydraulic conductivity	1.3×10^{-6} $ml/(min{\cdot}mmHg{\cdot}cm^2)$	[191]

$$V_{p,ha}(t)\frac{dC_{p,ha}(t)}{dt} = C_{phys}Q_{ha}(1-h_{phys}) - C_{p,ha}(t)\left(Q_{ha}(1-h_{ha}(t)) + Q_{c,ha}(t)\right) \quad (5.21)$$

$$V_{c,ha}(t)\frac{dC_{c,ha}(t)}{dt} = C_{phys}Q_{ha}h_{phys} - C_{p,ha}(t)\left(Q_{ha}h_{ha}(t) - Q_{c,ha}(t)\right) \quad (5.22)$$

$$V_{p,s}(t)\frac{dC_{p,s}(t)}{dt} = C_{p,pv}(t)(Q_{hs}+Q_{pv})(1-h_{pv}) + C_{p,ha}(t)Q_{ha}(1-h_{ha}(t)) + C_{p,hp}(t)Q_r(t) - C_{p,s}(t)Q_f(t) - C_{p,s}(t)\left(Q_{hv}(1-h_s(t)) + Q_{c,s}(t)\right) \quad (5.23)$$

$$V_{c,s}(t)\frac{dC_{c,s}(t)}{dt} = C_{c,pv}(Q_{hs}(t)+Q_{pv})h_{pv}(t) + C_{c,ha}(t)Q_{ha}h_{ha}(t) - C_{c,s}(t)\left(Q_{hv}h_s(t) - Q_{c,s}(t)\right) \quad (5.24)$$

$$V_{p,hp}(t)\frac{dC_{p,hp}(t)}{dt} = C_{p,s}(t)Q_f - C_{p,hp}(t)\left(Q_r(t)+Q_{c,hp}(t)\right) \quad (5.25)$$

$$V_{c,hp}(t)\frac{dC_{c,hp}(t)}{dt} = C_{c,hp}(t)Q_{c,hp} \quad (5.26)$$

$$\frac{dV_{p,x}(t)}{dt} = Q_{c,x} \quad (5.27)$$

$$\frac{dV_{c,x}(t)}{dt} = -Q_{c,x} \quad (5.28)$$

In vivo conductivity measurements

Animal model All actions in this study were performed in accordance with the protocol approved by the Ethical Commission of the Universitat Autònoma de Barcelona (authorization number CEEAH 2205/ DMAH 7633) following the European Directive 2010/63/EU on the protection of animals used for scientific purposes. A total of 5 procedures – one in each animal – were performed under general anesthesia on Landrace pigs (mean weight 57 kg).

Procedure Preoperative care and anesthesia were provided by fully trained veterinary staff. The anesthetic induction phase was performed with propofol (4 mg/kg i.v.) and maintained with isoflurane 1.5-2% and oxygen 100% mixture once the animal was endotracheally intubated. Oxygen saturation, arterial blood pressure, heart rate and capnography were monitored using a multiparametric monitor.

By midline laparotomy, after dissection of the hepatoduodenal ligament, extrahepatic portal vein catheterization was performed in order

to deliver either a hypersaline solution (NaCl at 20%) or an isotonic solution (NaCl 0.9%) in the control case. After exposure, the portal vein was dissected free and cannulated through a purse-string suture placed just cranial (approximately 1 cm) to the entry point of the cranial pancreaticoduodenal vein with a simple silastic catheter (dropper tube). The catheter was advanced cranial to a point just proximal to the main portal division and secured in place via the purse-string suture and a single stay suture. The solution volume employed in the procedures was injected by using a dropper while infusion durations were measured with a stop watch. Aiming to explore the conductivity dependence in both the amount of solution injected and the flow rate, different values were employed (see Table 5.3).

Table 5.3: Injection parameters employed in animal experiments.

Animal	NaCl (%)	Volume (ml)	Duration (s)	Flow (ml/min)
#1	20	100	113	53
#2	20	100	52	115
#3	20	120	60	120
#4	20	200	70	171
#5	0.9	500	120	250

Although the planned therapeutic technique involves hepatic vascular isolation, such strategy was not employed during this pilot study aiming to simplify the experimental setup. However, since rapid infusion of a high amount of HS could cause severe damage to the animal and a high disturbance of the normal blood flow [210] which could distort the study, it was decided to adopt a relatively simple approach to prevent those consequences. Specifically, in order to minimize the possible ionic and osmotic imbalance at systemic level caused by the HS, as recommended to manage hypernatremia [211], distilled water was simultaneously injected at the cava vein. Using an additional catheter with the same cannulation technique immediately cranial to entry point of the right renal vein and advanced cranial two centimeters. The amount of injected water was ten times the hypersaline volume in order to restore the NaCl concentration in the systemic blood.

Conductivity measurement It is possible to measure the impedance of a living tissue portion by inducing a known current through a pair of electrodes while measuring the resulting voltage drop across

them. In the presented study, the electrode setup consisted of two printed circuit boards (PCBs) with a circular gold electrode (20 mm diameter). The PCBs were mounted on a pincer clip so that the electrodes were securely placed at opposite sides of a hepatic lobule forming a fixed geometry. The electrodes were placed at a distal section of the lobule to avoid the potential influence of large intrahepatic blood vasculature. Electrical impedance was measured at a rate of five sweeps per second. The spectrogram consisted of six frequencies from 10 to 100 kHz. The excitation signal was a sinusoidal signal with 1 V amplitude applied to the tissue through a resistor in order to limit the peak current to a maximum of 500 μA. Both the injected current and the voltage drop over the tissue were simultaneously collected to compute the real and imaginary parts of the impedance using a data acquisition board (NI USB-6212, National Instruments) controlled by a virtual instrument (LabVIEW 8.1, National Instruments). The Cole model for bioimpedance can be employed to characterize the measured impedance ($Z(f)$) spectrogram with only four parameters: the hypothetical resistance at infinite (R_∞) and zero (R_0) frequencies, the characteristic time constant τ and the dimensionless parameter α [212].

$$Z(f) = R_\infty + \frac{R_0 - R_\infty}{1 + (j2\pi f\tau)^\alpha} \tag{5.29}$$

This equation was employed here to determine the hypothetical impedance magnitude at 0 Hz automatically fitting the equation (MATLAB R2014b, The MathWorks Inc.) to the experimental data by minimizing the least squares error.

Once the impedance at 0 Hz was obtained in equation 5.29, the conductivity at this frequency (σ_0) was calculated according to the geometric cell constant (K) of the measurement system as computed by means of a model based on Finite Element Method [212].

$$\sigma_0 = \frac{1}{R_0 K} \tag{5.30}$$

5.3.3 Results

According to the described formulation and the parameters of the Table 5.2, the physiological electrical conductivity of the plasma, blood and liver at 37°C is 2.03 S/m, 0.85 S/m and 0.09 S/m respectively.

Figure 5.9(a) shows the estimated evolution of the liver conductivity over the time. The simulation results show a fast increase at the beginning of the infusion mainly due to the presence of high conductivity medium on sinusoids (Figure 5.9(b)). Following that, the contribution of sinusoidal medium remains constant while the interstitial contribution – due to the filtration process and hepatocyte shrink – keeps growing until HS injection stops (Figure 5.9(c)). At this point, the rapid decrease in liver conductivity can be attributed to the replacement of the high conductivity sinusoidal content by systemic blood. Meanwhile, the high conductivity plasma at the interstitial space is arrested for a longer period of time, producing a remaining conductivity offset which requires longer periods to return to the physiological values.

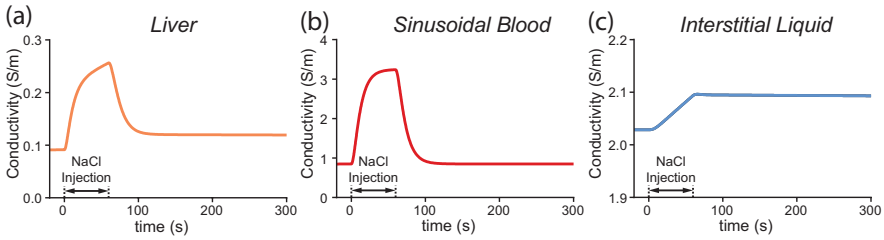

Figure 5.9: Temporal evolution of the computed electrical conductivity. Assessment of conductivity of the liver (a), the sinusoidal blood (b) and the interstitial liquid (c). Plots correspond with an injection of 2 ml/kg of 20% NaCl at 2 ml/(min·kg).

For an injected saline concentration of 20%, the model has two independent input parameters corresponding to the flow rate and the total amount of solution introduced. The effect of each of those inputs over the temporal evolution of the conductivity is shown in Figure 5.10. It can be observed that the maximum electrical conductivity achieved at the end of the HS injection highly depends on both the flow and the volume.

About the *in vivo* pilot study, it is important to note that only the electrical conductivity of the liver can be measured with the employed setup. The baseline electrical conductivity of the liver was very similar in all the animals (0.11 ± 0.02 S/m). As observed in computer simulations, conductivity progress always peaked just at the end of the injection. The maximum peak value was 0.44 S/m (animal #4) and corresponded with an injection of 3.8 ml/kg at 3.3 ml/(min·kg) (Figure 5.11(a)). Injection of a highly concentrated NaCl solution

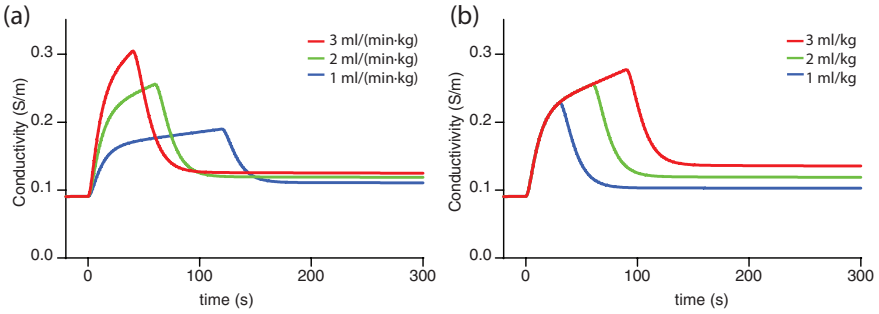

Figure 5.10: Effect of flow rate and volume of injected saline on the temporal evolution of electrical conductivity in the liver. Plots of (a) correspond with a fixed volume of 2 ml/kg of 20% NaCl, while plots in (b) correspond with a constant flow rate of 2 ml/(min·kg).

through portal vein produced a rapid increase of conductivity with time until the injection stops. At this point, a portion of the achieved conductivity increase slowly receded exponentially with time. However, the liver conductivity remained at a higher value than the basal one. In the control animal (animal #5), in which physiological saline solution (NaCl 0.9%) was injected, the conductivity of the liver did not show any variation, remaining at basal level (Figure 5.11(b)).

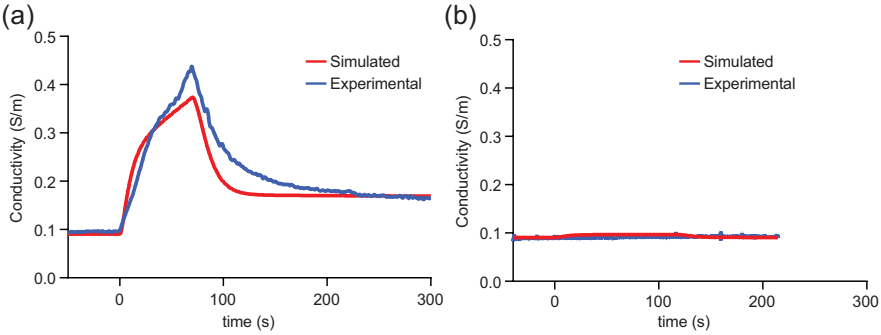

Figure 5.11: Temporal evolution of liver conductivity from simulations and experiments. (a) Temporal evolution in the case of an injection of 3.8 ml/kg (20% NaCl) at a flow rate of 3.3 ml/(min·kg). (b) Temporal evolution in case of injecting physiological saline solution (0.9% NaCl) which served as a control test.

Assessing with the model the resulting conductivity peak for a set of volumes and flows combinations, it is possible to obtain three-dimensional representation of the peak conductivity value within a range of flow rates and volumes (Figure 5.12). Those values can be

compared to the ones obtained during the *in vivo* pilot study in order to assess the goodness of fit of the proposed model in terms of relative error (Table 5.4).

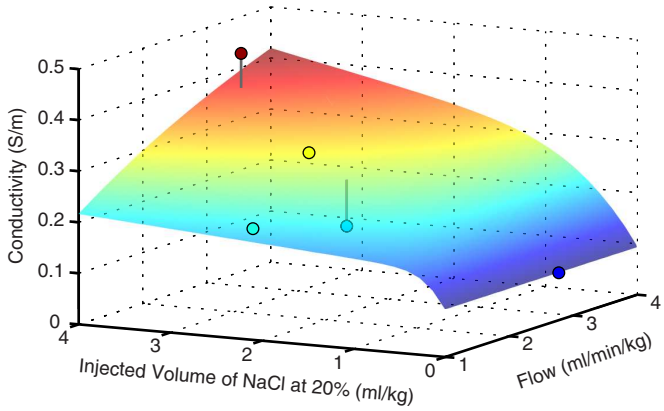

Figure 5.12: Dependence of conductivity peak on volume and flow of injected saline (20% NaCl). The surface represents the simulated values from the proposed mathematical model, while circles represent the five experimental results from the *in vivo* model. Gray lines denote the absolute error value between the values predicted by the model and those experimentally observed.

Table 5.4: Basal conductivity (σ_0) and peak conductivity (σ_p) values during the experimental procedures and comparison with computer simulations.

Animal	Volume 20% NaCl (ml/kg)	Flow Rate (ml/(min·kg))	Simulation		Experimental		Error	Error
			σ_0 (S/m)	σ_p (S/m)	σ_0 (S/m)	σ_p (S/m)	σ_0 (%)	σ_p (%)
#1	2.2	1.2	0.091	0.206	0.124	0.210	26.6	1.7
#2	1.9	2.2	0.091	0.266	0.109	0.178	16.5	49.7
#3	2.6	2.6	0.091	0.304	0.137	0.295	33.8	3.2
#4	3.8	3.3	0.091	0.373	0.093	0.444	2.5	15.8
#5	0.0	2.7	0.091	0.096	0.089	0.094	2.0	2.6

5.3.4 Discussion

In this study, a mathematical model of liver was developed aiming to assess the electrical conductivity of the tissue once hypertonic saline solution is introduced through portal vasculature. Our purpose was to formulate a mathematical model useful to continue with the development of a novel multi-nodule ablation technique based on electroporation.

According to the employed methodology, the physiological conductivity for blood would be 0.85 S/m, which is larger than the value commonly reported (about 0.65 S/m) [213] but close to the reported value in other experimental studies (0.76 S/m) [214]. Physiological values for liver conductivity at low frequency found in literature range widely from very low values (0.03 S/m) [132] to larger values (0.126 S/m) [185]. The physiological conductivity predicted by the model is 0.09 S/m, which is close to the commonly reported value (0.075 S/m) [212] and within the range of the basal conductivities, 0.11 ± 0.02 S/m (mean $\pm$ SD), obtained during the *in vivo* experiments reported here.

According to the results of the experimental study, the developed model is able to predict with an acceptable mean error (14.6%) the maximum conductivity of the liver once HS is portally injected. These results, together with the consistency of the basal conductivity results reported in the literature (previous paragraph), indicate the goodness of the model for our purposes. However, we deem the model could be further improved. In particular, we consider that a severe limitation of the model is that it assumes constant macroscopic volumes. In contrast, it is known that the liver acts as an expandable blood reservoir [215] and its compliance could hence play an important role. This factor should be incorporated in future models in order to predict the expected conductivity even in pathological states such as cirrhotic or fibrotic in which mechanical properties of the tissue differs from the normal ones.

The developed model accounts the increased blood viscosity in the sinusoids due to the high osmolarity of the HS. Such increase in viscosity raises the hydrostatic pressure in the sinusoids which in turn causes an excess of filtration/reabsorption flow thereby rapidly flushing out the original interstitial fluid. This would make the proposed model a useful tool not only for the particular case of HS injection but also for assessing the distribution of other hypertonic solutions such as high concentration contrasts [216].

Hypertonic saline solution has been extensively used in resuscitation of patients with traumatic brain injury [217]. Using 7.2% NaCl intravenously injected, it has been reported a safety dosage of 5 ml/kg of body weight without inducing hypernatremia [218]. Accordingly to this safety value, the maximum dosage at 20% NaCl would be 1.8 ml/kg. This amount is slightly below the maximum doses tried and proposed here for significantly increasing liver conductivity. There-

fore, some sort of countermeasure is required for safety in order to avoid severe pathophysiological effects, such as hyperchloremic acidosis or dilated coagulopathy [219]. For the presented pilot study parallel downstream administration of distilled water was a feasible and effective countermeasure to avoid acute dysfunctions at systemic level that could distort our study. However, the proposed electroporation technique should include a sort of liver isolation similar to the employed in the isolated hepatic perfusion (IHP) therapies [220].

Besides systemic effects, another source of concern is the potential tissue damage produced on the liver tissue itself due to the hypersaline injection. Nevertheless, according to literature, a direct intratisular injection of hypersaline solution at very high dosage (36.5% NaCl) it is required to produce small tissue damage [221]. And according to the presented model, at the maximum dosage employed during the *in vivo* experiments, interstitial concentration hardly reaches a concentration of 1% NaCl. Therefore hepatocellular damage due to portal injection of the hypersaline solution is not anticipated.

5.3.5 Conclusions

A mathematical model able to assess the resulting electrical conductivity of the liver when hypertonic saline solution is portally injected is presented. The model is able to estimate the time-space distribution of the solute within the different physiological parts of the organ.

The results show that the developed model is able to predict with an acceptable error (mean 14.6%) the maximum liver conductivity observed during the pilot *in vivo* study. The experiments were conducted on pigs where liver electrical conductivity was measured during injection of NaCl at 20% through the portal vein at different volumes and flow rates. The goodness of the model would make it useful not only for the particular case of hypersaline injection but also for other hypertonic solutions injections such as high concentration contrasts.

Both mathematical model and pilot *in vivo* results show the feasibility of increasing up to four times the conductivity of the healthy liver, which is suitable for the further development of the novel ablation modality based on electroporation.

5.3.6 Appendix

Estimation of physiological parameters

Most of the parameters employed in the model (Table 5.2) were extracted directly from the literature. However, some of the required parameters could not be found in past experimental studies and had to be estimated under some assumptions. In here it is described the processes for obtaining those estimations.

First, the model requires the physiological volume of blood in each vascular tree (i.e. portal, arterial and venous vasculature). Dimensional measurements of the intrahepatic vasculature were reported in [222] by using casting resin. Based on these data – simplifying vessels as tubes – the total volume of each tree was calculated (81.6 ml for the arterial tree, 236.7 ml for the portal tree and 288.0 ml for the venous tree). According to the liver weight employed in the experimental study (1.9 kg) and the liver density (1070 kg/m^3 [209]) the vasculature volume ratios with respect to the total liver volume were calculated: 4.6% for the arterial tree, 13.3% for portal tree and 16.2% for the venous tree.

Second, no data was found regarding the contact surface ($S_{c,hp}$) between the hepatocytes and the interstitial space. Considering the sinusoids as tubes of radius r_s (5 μm [206]), it was possible to calculate the total length of the sinusoids per unit of liver volume (8.89×10^8 m/m^3) required to hold the sinusoidal blood (10.6% of parenchyma volume (V_P) [208]). The interstitial space was then modeled as an annular region around the sinusoids with their same length. The width of this region (1.05 μm) was determined by the physiological interstitial volume ($V_{p,hp}$) (4.9% of parenchyma volume [208]). Finally, the interface between the hepatocytes and the interstitium per unit of liver volume was assumed to be the outer surface of the cylinder formed by the sinusoids and the surrounding interstitial ring resulting in 337.9 cm^2/ml.

Nomenclature

The mathematical model described in this work uses several parameters for its definition. The employed nomenclature for this parameters follows the same structure. The main symbol (Table 5.5) indicates the defined magnitude for the parameter, whereas the subscript or subscripts (Table 5.6) indicate the anatomical location or state which is

intended to be represented. Table 5.7 lists the individual description for each of the parameters employed in the model.

Table 5.5: Description of magnitudes used in the model.

Symbol	Description
C	Concentration of solute
h	Hematocrit
K_f	Capillary filtration coefficient
L_c	Membrane hydraulic conductivity
P	Hydrostatic pressure
Q	Flow
R	Flow resistance
S_c	Surface between cells and extracellular plasma
T	Temperature
V	Volume
μ	Blood viscosity
Π	Osmotic pressure
ρ	Density
σ	Electrical conductivity

Table 5.6: Description of subscripts used in the model.

Subscript	Description
L	Liver
P	Parenchyma
ha	Hepatic artery
hp	Hepatocellular plates
pv	Portal vein
hv	Hepatic vein
s	Sinusoids
hs	Hypertonic solution
c	Cells
p	Plasma
$phys$	Physiological

Table 5.7: Description of parameters used in the model.

Symbol	Description
$C_{c,ha}$	Concentration in RBC at hepatic artery
$C_{c,hp}$	Concentration in hepatocites at hepatocellular plate
$C_{c,pv}$	Concentration in RBC at portal vein
$C_{c,s}$	Concentration in RBC at sinusoids
C_c	Concentration of solute at the cells
C_{hs}	Concentration of hypertonic solution
$C_{p,ha}$	Concentration of plasma at hepatic artery
$C_{p,hp}$	Concentration of plasma at hepatocellular plate
$C_{p,pv}$	Concentration of plasma at portal vein
$C_{p,s}$	Concentration of plasma at sinusoids
C_p	Concentration of solute in plasma
C_{phys}	Physiological concentration
h_{ha}	Hematocrit value at hepatic artery
h_{phys}	Hematocrit value at physiological state
h_{pv}	Hematocrit value at portal vein
h_s	Hematocrit value at sinusoids
$L_{c,ha}$	Membrane hydraulic conductivity at hepatic artery
$L_{c,hp}$	Membrane hydraulic conductivity at hepatocellular plates
$L_{c,pv}$	Membrane hydraulic conductivity at portal vein
$L_{c,s}$	Membrane hydraulic conductivity at sinusoids
$P_{hv,phys}$	Hydrostatic pressure at the beginning of the hepatic vein at physiological state
P_{hv}	Hydrostatic pressure at the beginning of the hepatic vein
P_i	Hydrostatic pressure at the interstitial space
$P_{s,phys}$	Hydrostatic pressure at the beginning of the sinusoids at physiological state
P_s	Hydrostatic pressure at the beginning of the sinusoids
$Q_{c,ha}$	Flow of water leaving from cells at hepatic artery
$Q_{c,hp}$	Flow of water leaving from cells at hepatocellular plate
$Q_{c,pv}$	Flow of water leaving from cells at portal vein
$Q_{c,s}$	Flow of water leaving from cells at sinusoids
Q_f	Flow of filtration from sinusoids to interstitium
Q_{hs}	Flow of hypertonic solution
Q_{hv}	Flow of blood at the hepatic vein
Q_{pv}	Flow of portal vein
Q_r	Flow of reabsorption from interstitium to sinusoids
$Q_{s,phys}$	Flow of blood through sinusoids at physiological state
Q_s	Flow of blood through sinusoids

Symbol	Description
$R_{s,phys}$	Flow resistance of sinusoids at physiological state
$S_{c,ha}$	Cellular membrane surface at hepatic artery
$S_{c,hp}$	Cellular membrane surface at hepatocellular plates
$S_{c,pv}$	Cellular membrane surface at portal vein
$S_{c,s}$	Cellular membrane surface at sinusoids
$V_{c,ha}$	Volume of RBC at hepatic artery
$V_{c,hp}$	Volume of hepatocytes at hepatocellular plate
$V_{c,pv}$	Volume of RBC at portal vein
$V_{c,s}$	Volume of RBC at sinusoids
$V_{p,ha}$	Volume of plasma at hepatic artery
$V_{p,hp}$	Volume of plasma at hepatocellular plates
$V_{p,pv}$	Volume of plasma at portal vein
$V_{p,s}$	Volume of plasma at sinusoids
V_P	Volume of the parenchyma
V_s	Volume of the sinusoids
μ_{phys}	Blood viscosity at physiological state
μ_s	Blood viscosity at sinusoids
σ_{eff}	Effective electrical conductivity
σ_L	Electrical conductivity of liver
$\sigma_{p,hp}$	Electrical conductivity of plasma at hepatocellular plates (interstitial liquid)
$\sigma_{p,s}$	Electrical conductivity of sinusoidal plasma
σ_{si}	Electrical conductivity of sinusoids and interstitium liquid
σ_{solv}	Conductivity of the solvent
σ_p	Electrical conductivity of plasma
σ_s	Electrical conductivity of sinusoidal blood

5.4 Irreversible electroporation of a large portion of the liver

5.4.1 Introduction

According to the performed simulations of the *STEP-HI* technique (section 5.2), the IRE thresholds of both healthy and tumor tissues are critical parameters for the treatment feasibility. In order to make a step forward in the development of the technique, an *in vivo* experiment was designed to determine the minimum electric field required to treat the tumorous tissue as well as the maximum field bared by the healthy liver. As described in more detail in the following methods section, immunodeficient nude mice with an implanted tumor in the left lobule were treated. The two most left lobules where electroporated at the same time using parallel plate electrodes to generate a homogeneous electric field. During the firsts experiments, an intensive protocol (100 pulses of 100 μs at 2000 V/cm delivered at 1 Hz) was selected to ensure the ablation of the tumors.

Surprisingly, a sudden death of the animals was observed between the followings 15 minutes and few hours after the treatment. It must be pointed out that none of the animals died during the pulse application, but they were lethargic and tachypneic immediately after the treatment application.

Cell membrane is in charge of keeping the ionic content inside the cell. At physiological state, a high concentration of potassium ions (about 140 mmol/l) are present inside the cells which highly differs form the extracellular medium concentration (around 4 mmol/l) [223]. An acute disturbance of extracellular potassium levels entails severe consequences for the normal cell homeostasis [224]. In highly effective chemotherapeutic therapies, the fast killing process of tumor cells releases the intracellular content into the bloodstream which leads to an electrolyte and metabolic disturbance inducing the so called tumor lysis syndrome [225].

Since electroporation produces high permeabilization of the membrane structure, the intracellular ionic content outflows by diffusion gradient [226]. Coarse calculations can be performed aiming to elucidate the disturbance magnitude caused during the pilot experiments. For a mouse 25 g mouse, the liver organ is about 1.7 g with 1.2 ml of intracellular liquid [227]. The two segments of the left liver represents nearly 40% of its volume, hence, releasing the whole intracellular content into the bloodstream results in a potassium bolus

of 105 μg $[K^+]$/g of the animal weight. For humans and rabbits, 35 μg $[K^+]$/g has been reported as a fatal bolus of potassium [228].

Based on this approximations and the observed symptomatology after the treatments, the following hypotheses was proposed: Potassium release after IRE of large tissue volumes can compromise the life of the subject.

The understanding of this fatal outcomes was prioritized over the initial goal of the study due to its clinical relevance. In order to prove the formulated hypothesis, systemic potassium levels were measured after liver electroporation. A group of animals was treated with an intensive anti-hyperkalemia therapy, trying to manage the possible ionic unbalance. In addition, the same treatments in a subset of immunocompetent animals were conducted due to the concerns regarding the sensibility of inmunodepressed mice to IRE treatments [88].

5.4.2 Materials and methods

All aspects of this study were performed as part of an animal research protocol, in accordance with the guidelines approved by the Government of Catalonia's Animal Care Committee (procedure FBP-13-1474, DAAM: 7016) following the European Directive 2010/63/EU.

Animal model

Two strains of six-week-old male mice (n=85), immunodeficient athymic-nude (Harlan Laboratories, Inc.) and immunocompetent C57-Bl6 (Charles River Laboratories, Inc.) were acquired and maintained under standard conditions with a laboratory diet and water *ad libitum*.

Tumor model

The KM12C human colon cancer cell line was implanted in immunodeficient mice (n=55). Tumors subcutaneously implanted and passaged in nude mice were extracted to prepare tumor fragments of $2\times2\times2$ mm^3 and then implanted. Animals were anesthetized with a mixture of isofluorane and inhaled oxygen and analgesia was provided with buprenorphine (0.05-0.1 mg/kg s.c.) and meloxicam (1-3 mg/kg s.c.). After anesthesia, a subxiphoid laparotomy was performed and the left lobe of the liver exposed. The tumor was stitched to the hepatic capsule using a monofilament suture of 6/0 prolene. The abdominal muscle layer was closed with a running suture of vicryl 5/0,

and the skin with a single silk suture. Following initial implantation, 15 days were allowed for tumor growth.

Irreversible electroporation treatment

The IRE procedure was performed employing custom pulse generator and applicators. After exposing the liver, parallel plate electrodes were placed comprising the two segments of the left liver (Figure 5.13). A partially conductive gel (Aquasonic 100, Parker Laboratories) was used to fill the air gaps between the two parallel plates, thus, improving electric field uniformity [121].

Three different magnitudes of electric field were applied: 2000 V/cm, 1000 V/cm and 0 V/cm (sham operated). The generator was programmed to deliver ten sequences of ten pulses with duration of 100 μs and repetition frequency of 1 Hz. There was a 10 s time gap between the ten pulses sequences to avoid a possible thermal damage.

During the first 72 h after surgery, all animals were given two additional doses of buprenorphine (0.05-1 mg/kg s.c.) and meloxicam (1-3 mg/kg s.c.), spaced out over 12 h increments.

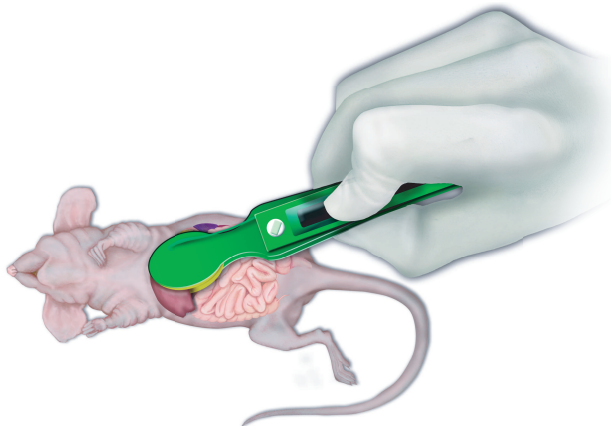

Figure 5.13: Illustration of the anterior view showing the plate electrodes placement on the targeted hepatic lobe of a mice.

Pharmacological therapy against hyperkalemia

Prior to surgery, the set of animals treated with the pharmacological therapy against hyperkalemia were intraperitoneally pre-hydrated with 200 μL of 0.9% NaCl solution every 24 h for two consecutive days. Calcium gluconate was injected in the preoperative care in two

boluses, both intravenously (i.v.) and intraperitoneally (i.p.) at a dose of 100 mg/kg [229]. To prevent hyperkalemia, a furosemide i.v. bolus (4 mg/kg) was administered and during anesthesia induction oxygen was mixed with inhaled salbutamol (100 μg). After the procedure, sodium bicarbonate ($NaHCO_3$) i.p. was administered before the closure of the abdominal wall at a dose of 1 mEq/kg [229].

Analytical tests at 10 min and 6 h post-IRE were performed to quantify blood electrolytes with a blood analyzer device (i-STAT, Abbott Point of Care Inc.). Blood samples were obtained by a single puncture in the saphena vein.

Estimation of electroporated volume

The following parameters were evaluated in the liver samples harvested during the *in vivo* experiments: total liver weight, electroporated liver weight, total liver volume and electroporated liver volume. A precision scale was used to determine the weight. Volume was measured by placing the tissue samples in a laboratory graduated cylinder filled with water and quantifying the displaced volume.

Statistical Analysis

Statistical analyses were performed with a specialized software package (SPSS v.19, IBM Inc.). In a conservative approach non-parametric tests were used. Namely, Chi-Square test has been used to compare survival outcomes and the two-tailed Mann-Whitney U test for potassium results. Tests were considered statistically significant with a p-value < 0.05 and values expressed as mean $\pm$ standard deviation.

5.4.3 Results

Table 5.8 summarizes the data collected during the *in vivo* experiments. The results point out the harmless of the intervention procedure but reveal a high mortality in the first 24 hours (48.6%) of animals treated with IRE. This mortality shows different ratios according to the electric field magnitude and the pharmacological therapy. The post-IRE potassium level corresponds to the maximum value of potassium measured between the 10 min and 6 hours after the procedure. The harvested liver samples show a mean volume of 1.45 $\pm$ 0.31 ml and an electroporated volume of 0.55 $\pm$ 0.21 ml corresponding to a 38% of the liver.

Table 5.8: Classification of the different groups of animals.

Strain	Electric Field (V/cm)	Anti-hyperkalemia therapy	n	Alive	Post-IRE [K] (mmol/L)
Athymic-Nude	0	No	15	15	7.46 ± 1.33
Athymic-Nude	1000	No	11	8	9.61 ± 3.22
Athymic-Nude	2000	No	9	0	12.76 ± 4.68
Athymic-Nude	2000	Yes	20	16	7.68 ± 1.42
C57-B16	2000	No	8	2	7.98 ± 1.30
C57-B16	2000	Yes	22	10	7.77 ± 2.18

Effect of the electric field magnitude

Figure 5.14 shows the survival outcomes and post-treatment potassium levels at different electric field magnitudes in Atymic-Nude mice without anti-hyperkalemia pharmacological therapy. The survival rate shows statistical differences between each of the assessed magnitudes (Chi-square test: 0-1000 V/cm (p=0.031), 0-2000 V/cm (p< 0.001), 1000-2000 V/cm (p=0.001)). These significances reflect the relation between the treatment intensity and the survival results. This dependency is also observed when comparing the potassium levels after these treatments (Mann-Whitney U test: 0-1000 V/cm (p=0.029), 0-2000 V/cm (p=0.037), 1000-2000 V/cm (p=0.28)).

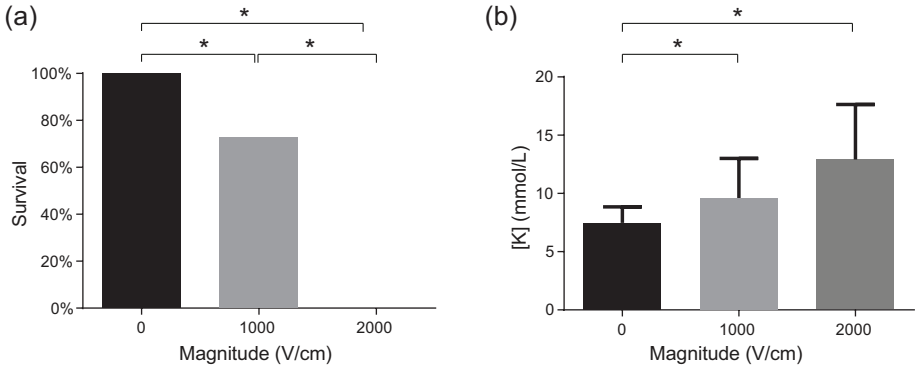

Figure 5.14: Results of the experiments performed with inmunodepressed mice without anti-hyperkalemia therapy. (a) Survival rate according to the electric field magnitude. (b) Post-IRE potassium concentration according to the electric field magnitude.

Effect of the anti-hyperkalemia pharmacological therapy

To ascertain the efficacy of the anti-hyperkalemia therapy, we analyzed separately the survival rate of the animals that received maximum treatment intensity (2000 V/cm) plus anti-hyperkalemia therapy and those who did not (Figure 5.15). The results show a statistical significance in the mortality once anit-hyperkalemia therapy is administrated (Chi-Square test: $p<0.001$). Independently, the post-treatment potassium is also dependent on the pharmacological therapy showing a significant reduction of this value in case of pharmacological management (Mann-Whitney U test ($p=0.012$)).

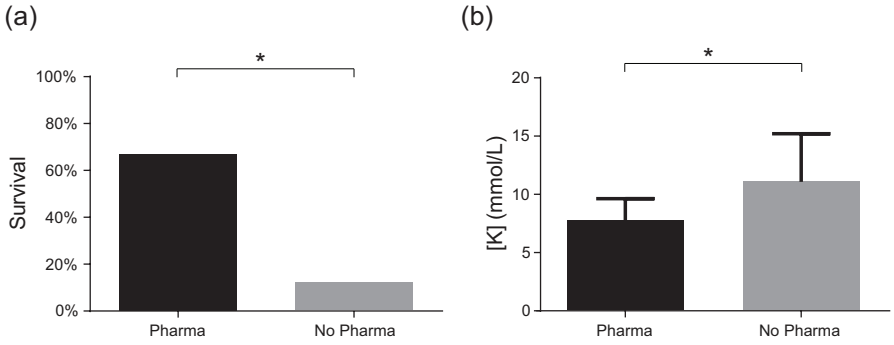

Figure 5.15: Results of the experiments performed with 2000 V/cm. (a) Survival rate according to the pharmacological administration. (b) Post-IRE potassium concentration according to the pharmacological administration.

Relevance of potassium in death

Finally, the direct relationship between the survival outcomes and the post-treatment potassium levels was tested. Figure 5.16 shows the potassium levels of both survival and expired animals regardless the electroporation treatment, strain or pharmacological therapy. The statistical significance between both groups (Mann-Whitney U ($p=0.007$)) reveals the direct relationship between the potassium level and the animal survival.

5.4.4 Discussion

The experimental results show a high rate (48.6%) of mortality within the first 24 hours after the application of IRE treatments over a large volume of the liver. The correlation between the electric field strength and the survival rate suggests the direct implication of the electropo-

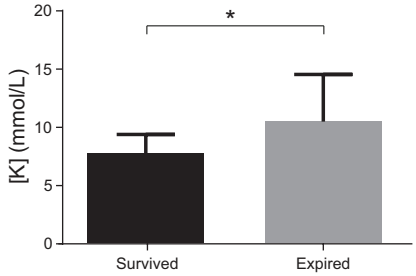

Figure 5.16: Post-IRE potassium concentration according to the survival outcomes of the whole set of animals.

ration phenomenon in the observed sudden deaths. The rising potassium levels as the applied magnitude is increased (Figure 5.14(b)) hint the plausibility of the planned hypothesis. Furthermore, administrating the palliative anti-hyperkalemia therapy results in a reduction of both the fatal outcomes and post-IRE potassium levels (Figure 5.15). Considering this results, the potassium implication in the animals death gain strength. This suspicion is further reinforced since the potassium measured after the procedure (regardless the treatment group) shows significant differences between survival animals (7.7 $\pm$ 1.651 mmol/L) and those which eventually die (10.2 $\pm$ 4.1 mmol/L). The observed outcomes agree with the reported potassium limits in mice (5.1 - 10.4 mmol/L) [229]) and fit with the suggested hypothesis.

Despite the fatal outcomes observed, irreversible electroporation has repeatedly demonstrated its safety use in clinics [230; 231; 232; 233; 234; 235] for moderate ablation volumes (lower than 3.5 cm). A single study has reported slight metabolic acidosis and hyperkalemia in small fraction of patients (14.3%) who underwent ablation of very large tumors [236]. This observation perfectly fits with the hidden hypothesis where: the larger the ablation volume the greater the disturbances are expected.

The current electroporation technology limits the capabilities to ablate larger volumes, thus, it avoids the occurrence of a fatal ionic imbalance in clinical IRE treatments. Nonetheless, the upcoming generation of electroporation devices – such as the one presented in Chapter 4 – could entail a significant metabolic acidosis and hyperkalemia. In this case, when a large volume of tissue is intended to be treated with IRE, measures such as intensive patient monitoring and palliative pharmacological therapy should be adopted.

5.5 Conclusions

This chapter presents a novel ablative approach based on electroporation phenomenon which is able to selectively affects the tumor nodules within the liver. This technique, referred here as *STEP-HI*, relies on increasing the healthy liver conductivity by means of hypertonic saline solution.

The exploratory simulations of the treatment covered in the first section of the chapter hint the technique's feasibility as long as the electrical conductivity of the liver is increased enough to magnify the electric field in cancerous tissue over its IRE threshold. These simulations show the existence of a treatment magnitude interval where successful results can be achieved. The width of this magnitude window increases with a higher conductivity enhancement but could decreases depending to the geometry, conductivity and IRE threshold of the tumor. Consequently, it is desired to achieve as much conductivity increase as possible by means of the hypersaline solution.

The capability of hypertonic saline solutions to increase the liver conductivity has been assessed in the second section of this chapter. First, a mathematical model was developed to predict the temporal evolution of the electrical conductivity of the liver when HS is injected through the vasculature. Since no experimental data were available, a pilot experimental study in pigs was performed. Both mathematical model and pilot *in vivo* results show the feasibility of increasing up to four times the conductivity of the healthy liver, which is an enhancement capability suitable for the further development of the *STEP-HI* technique.

The last section presents the unexpected findings observed during the exploration of the electroporation thresholds. This study shows a sudden death of the animals undergoing an IRE ablation of a large volume of tissue. The electrolyte measurements after the treatments, reveals that the massive outflowing of potassium form the electroporated cells could compromise the life of the subject. Current clinical electroporation treatments are not extensive enough to produce such a fatal outcome. However, the incoming improvements in electroporation technologies foresee the appearance of this situation in the near future. For this situations, where a large volume of tissue is intended to be ablated by IRE, a countermeasure against the possible potassium imbalances, such as the pharmacological one employed in this study, should be used.

Overall, this chapter presents the first steps toward the development of the *STEP-HI* electroporation technique. It has been demonstrated the theoretical feasibility using numerical simulations, which are supported by experimental data. This work has also identified some potential threads from the safety point of view. Namely, the electrolyte disruption induced by the injected saline along with the potassium released by the ablated cells could compromise the life of the patient. Nonetheless, the hepatic perfusion isolation needs to be considered as an effective measure against both adverse conditions. Further studies should be performed in the future to make the technique feasible as therapeutic option.

Chapter 6

Conclusions

6.1 General conclusions

This dissertation has been focused on the development and evaluation of non-thermal electrical methods for cancer treatment. More specifically, the work presented here revolves around the exploration of non-focal approaches able to treat tumors without addressing them individually.

This work starts in Chapter 3 presenting the first independent animal study where TTFields were used to treat solid tumors. This study arose from the hypothesis that the permanent exposition to mild hyperthermia produced by Joule heating is the responsible of the reported treatment efficacy. Our study revealed no capability of TTFields to halt the disease progression, only slight decrease in the growth rate has been observed when chemotherapy and TTFields are combined. Contrary to our hypothesis, the slight synergy between the applied alternating electric field and the chemotherapeutic agent is non-thermally mediated. Accounting the weak results of TTFields reported here, it has a marginal applicability being relegated to a palliative therapy.

The remaining work presented in this dissertation pursuits the development of new tools and methods for electroporation-based treatments. We first proposed a novel modular structure for electroporation generators. The design, presented in Chapter 4, was conceived to exhibit a high flexibility and scalability in order to fulfill the vast majority of the current and future electroporation applications. A functional prototype was implemented in order to prove the versatility of the proposed topology. The assessment of the generated pulses in biological tissue was carried out in tubers. A remarkable contribution has been done regarding the observation method, which allows faster and three-dimensional evaluations of the IRE outcomes. The good performance of the scaled-down prototype supports the suitability of the proposed topology for the upcoming generation of pulse devices for electroporation.

Taking advantage of the improved pulse generator capabilities, in Chapter 5 we presented a novel electroporation technique able to change the paradigm of treatment for spread tumors in liver. This technique, coined as *STEP-HI*, consists in the injection of high conductivity solutions towards the characteristic liver blood supply. It enhances the electroporation effects over the tumorous nodules, while preserving the effects on the healthy parenchyma.

The feasibility of this approach was firstly assessed by numerical simulations using a set of assumptions regarding the salinized liver conductivity. The results of these simulations show the feasibility of the technique as long as the conductivity in the healthy parenchyma is increased enough.

In order to estimate the conductivity effect of saline injection in portal vasculature, a mathematical model was developed. This model uses a compartmental pharmacokinetic model of the liver to assess the distribution of Na^+ and Cl^- ions within the different structures of the organ. Additionally, according to the high concentration of the proposed saline solutions (NaCl 20%) additional considerations were taken from the literature to represent the osmotic interactions. The resulting electrical conductivity of the liver was determined based on the estimated distribution of ions in the different organ structures. Since no data were available for the model assessment, a pilot *in vivo* study was carried out in pigs. The goodness of conductivity increase in both mathematical and *in vivo* confirms the efficacy of hypertonic saline solution to globally increase the conductivity of the tissue. However, the large amount of exogenous sodium chloride introduced during the procedure must be carefully managed for patients safety in order to avoid any possible systemic hypernatremia or electrolyte imbalance.

Finally, the electric field thresholds of liver and tumor tissue – a relevant value for the success of the STEP-HI technique – were studied. An *in vivo* experiment was performed in mice in which a large portion of the organ was electroporated. The preliminary results show a high rate of mortality after the IRE ablation. This both interesting and worrisome outcomes were further investigated under the hypothesis that the release of inner content of electroporated cells could produce a fatal bolus of potassium. The statistical analysis of survival and electrolyte levels after the procedure confirms the planned hypothesis. We conclude that the current electroporation therapies – where relative small volumes tissue are ablated –, can be considered as safety. Nonetheless, dangerous metabolic acidosis and hyperkalemia could be manifested in the future if larger ablation procedures are performed.

6.2 Future perspective

The non-thermal electrical methods for cancer treatment remains at the early stages of development. The non-focal approaches explored

here are even less mature, therefore, significant further efforts should be taken to make the technique a reliable option for cancer patients.

On the one hand, the lower effect over the disease progression, manifested by the TTFields technique, discourage the performance of further studies as a primary therapy. Instead, basic studies should be carried out in order to move forward in the understanding of the physiological response. The insight into the phenomenon responsible of the synergy between the low magnitude electric fields and the chemotherapeutic agent could results in a useful therapeutic option in case where no other treatment are possible.

On the other hand, electroporation-based therapies are gaining popularity among the clinicians as an effective tool for tissue ablation. Thanks to the unique features, electroporation stand out over the current armamentarium against cancer. Yet, the successful results still show some limitations regarding the lesion size capabilities. We purpose a novel topology able to disrupt the current technical barriers. The upcoming efforts should be taken in the development of a robust and reliable device able to be employed in clinical environments, ensuring the safety of both patients and users. This next generation of pulse device could represents the final push toward the consolidation of electroporation-based methods as a primary therapy for tumor ablation.

A large part of the work presented in this dissertation concerns the development of the STEP-HI technique as a new non-focal electroporation technique for liver tumors. Despite the several steps completed by this work there is still a long way to go on the road to the clinical treatment. The forthcoming steps should still face both the assessment of feasibility and safety of the treatment. As for the feasibility, *in vivo* experiments should be performed where the both liver and tumor electrical conductivity are simultaneously measured during the hypersaline injection. These experiments are critical in order to validate the independent manipulation of tumor and liver conductivities. Furthermore, the electric field thresholds for both healthy and tumorous tissue should be defined for the IRE protocol planned to be used. New numerical simulations should be carried out updating the exploratory parameters with the ones experimentally obtained. In addition, as treatments in high conductive tissues entails high electrical currents, the temperature increases due to Joule heating should be considered. On the other hand, further experiments regarding the safety of the procedure are required to prevent any harmful systemic

effects. The isolation of liver vasculature could be a good option to avoid both hypernatremia and hyperkalemia on this therapy.

Overall, the non-focal approach for non-thermal electrical treatments is still in its early development. Further efforts are required in order to become a treatment option for patients unresponsive or untreatable with current standards of care.

Bibliography

[1] L. A. Torre, F. Bray, R. L. Siegel, J. Ferlay, J. Lortet-tieulent, and A. Jemal, "Global Cancer Statistics, 2012," *CA: a cancer journal of clinicians.*, vol. 65, no. 2, pp. 87–108, 2015.

[2] L. Rahib, B. D. Smith, R. Aizenberg, A. B. Rosenzweig, J. M. Fleshman, and L. M. Matrisian, "Projecting cancer incidence and deaths to 2030: The unexpected burden of thyroid, liver, and pancreas cancers in the united states," *Cancer Research*, vol. 74, no. 11, pp. 2913–2921, 2014.

[3] C. E. DeSantis, C. Chieh Lin, A. B. Mariotto, R. L. Siegel, K. D. Stein, J. L. Kramer, R. Alteri, A. S. Robbins, and A. Jemal, "Cancer Treatment and Survivorship Statistics, 2014," *CA Cancer J Clin*, vol. 64, pp. 252–271, 2014.

[4] S. Stättner, F. Primavesi, V. S. Yip, R. P. Jones, D. Öfner, H. Z. Malik, S. W. Fenwick, and G. J. Poston, "Evolution of surgical microwave ablation for the treatment of colorectal cancer liver metastasis: review of the literature and a single centre experience," *Surgery today*, vol. 45, no. 4, pp. 407–415, 2015.

[5] B. Jeremić and G. M. Videtic, "Chest Reirradiation With External Beam Radiotherapy for Locally Recurrent Non-Small-Cell Lung Cancer: A Review," *International Journal of Radiation Oncology*Biology*Physics*, vol. 80, no. 4, pp. 969–977, jul 2011.

[6] K. D. Miller, R. L. Siegel, C. C. Lin, A. B. Mariotto, J. L. Kramer, J. H. Rowland, K. D. Stein, R. Alteri, and A. Jemal, "Cancer treatment and survivorship statistics, 2016." *CA: a cancer journal for clinicians*, vol. 66, no. 4, pp. 271–89, 2016.

[7] R. Stupp, M. E. Hegi, M. R. Gilbert, and A. Chakravarti,

"Chemoradiotherapy in malignant glioma: standard of care and future directions." *Journal of clinical oncology : official journal of the American Society of Clinical Oncology*, vol. 25, no. 26, pp. 4127–36, sep 2007.

[8] L. E. Schnipper, N. E. Davidson, D. S. Wollins, C. Tyne, D. W. Blayney, D. Blum, A. P. Dicker, P. A. Ganz, J. R. Hoverman, R. Langdon, G. H. Lyman, N. J. Meropol, T. Mulvey, L. Newcomer, J. Peppercorn, B. Polite, D. Raghavan, G. Rossi, L. Saltz, D. Schrag, T. J. Smith, P. P. Yu, C. A. Hudis, and R. L. Schilsky, "American Society of Clinical Oncology statement: A conceptual framework to assess the value of cancer treatment options," *Journal of Clinical Oncology*, vol. 33, no. 23, pp. 2563–2577, 2015.

[9] D. E. Abbott, C.-W. D. Tzeng, R. P. Merkow, S. B. Cantor, G. J. Chang, M. H. Katz, D. J. Bentrem, K. Y. Bilimoria, C. H. Crane, G. R. Varadhachary, J. L. Abbruzzese, R. a. Wolff, J. E. Lee, D. B. Evans, and J. B. Fleming, "The cost-effectiveness of neoadjuvant chemoradiation is superior to a surgery-first approach in the treatment of pancreatic head adenocarcinoma." *Annals of surgical oncology*, vol. 20 Suppl 3, pp. S500–8, 2013.

[10] N. Carelle, E. Piotto, A. Bellanger, J. Germanaud, A. Thuillier, and D. Khayat, "Changing patient perceptions of the side effects of cancer chemotherapy," *Cancer*, vol. 95, no. 1, pp. 155–163, 2002.

[11] I. C. Henderson, D. A. Berry, G. D. Demetri, C. T. Cirrincione, L. J. Goldstein, S. Martino, J. N. Ingle, M. R. Cooper, D. F. Hayes, K. H. Tkaczuk, G. Fleming, J. F. Holland, D. B. Duggan, J. T. Carpenter, E. Frei, R. L. Schilsky, W. C. Wood, H. B. Muss, and L. Norton, "Improved outcomes from adding sequential paclitaxel but not from escalating doxorubicin dose in an adjuvant chemotherapy regimen for patients with node-positive primary breast cancer," *Journal of Clinical Oncology*, vol. 21, no. 6, pp. 976–983, 2003.

[12] R. L. Bare and F. M. Torti, "Endocrine therapy of prostate cancer," *Cancer Treat Res*, vol. 94, no. June, pp. 69–87., 1998.

[13] M. Untch and C. Thomssen, "Clinical Practice Decisions in Endocrine Therapy," *Cancer Investigation*, vol. 28, no. sup1, pp. 4–13, jul 2010.

[14] T. A. Waldmann, "Immunotherapy: past, present and future," *Nature medicine*, vol. 9, no. 3, pp. 269–277, 2003.

[15] L. Naldini, "Gene therapy returns to centre stage," *Nature*, vol. 526, no. 7573, pp. 351–360, 2015.

[16] S. A. Rosenberg, N. P. Restifo, J. C. Yang, R. A. Morgan, and M. E. Dudley, "Adoptive cell transfer: a clinical path to effective cancer immunotherapy," *Nature Reviews Cancer*, vol. 8, no. 4, pp. 299–308, apr 2008.

[17] G. Goel and W. Sun, "Cancer immunotherapy in clinical practice - the past, present, and future," *Chinese Journal of Cancer*, vol. 33, no. 9, pp. 445–457, sep 2014.

[18] K. P. Charpentier, "Irreversible electroporation for the ablation of liver tumors: are we there yet?" *Archives of surgery (Chicago, Ill. : 1960)*, vol. 147, no. 11, pp. 1053–61, 2012.

[19] H. Yu and C. Burke, "Comparison of Percutaneous Ablation Technologies in the Treatment of Malignant Liver Tumors," *Seminars in Interventional Radiology*, vol. 31, no. 212, pp. 129–137, 2014.

[20] M. Ahmed, C. L. Brace, F. T. Lee, and S. N. Goldberg, "Principles of and Advances in Percutaneous Ablation," *Radiology*, vol. 258, no. 2, pp. 351–369, 2011.

[21] M. Trujillo, Q. Castellví, F. Burdío, P. Sánchez Velazquez, A. Ivorra, A. Andaluz, and E. Berjano, "Can electroporation previous to radiofrequency hepatic ablation enlarge thermal lesion size? A feasibility study based on theoretical modelling and in vivo experiments." *International journal of hyperthermia : the official journal of European Society for Hyperthermic Oncology, North American Hyperthermia Group*, vol. 29, no. 3, pp. 211–8, 2013.

[22] N. Goldberg and K. K. Tanabe, "Treatment of Intrahepatic Radiofrequency Ablation Correlation Malignancy with," *Most*, pp. 2452–2463, 2000.

[23] B. Rubinsky, "Cryosurgery." *Annual review of biomedical engineering*, vol. 2, pp. 157–87, jan 2000.

[24] E. VanSonnenberg, W. McMullen, and L. Solbiati, *Tumor Ablation: Principles and Practice*. Springer Science, 2008.

[25] T. Livraghi, L. Solbiati, M. F. Meloni, G. S. Gazelle, E. F. Halpern, and S. N. Goldberg, "Treatment of focal liver tumors with percutaneous radio-frequency ablation: complications encountered in a multicenter study." *Radiology*, vol. 226, no. 2, pp. 441–51, 2003.

[26] N. Finsen, "Phototherapy," 1901.

[27] R. R. Allison and C. H. Sibata, "Oncologic photodynamic therapy photosensitizers: A clinical review," *Photodiagnosis and Photodynamic Therapy*, vol. 7, no. 2, pp. 61–75, 2010.

[28] M. B. Vrouenraets, G. W. M. Visser, G. B. Snow, and G. A. M. S. van Dongen, "Basic principles, applications in oncology and improved selectivity of photodynamic therapy." *Anticancer research*, vol. 23, no. 1B, pp. 505–22, 2003.

[29] E. Nilsson, H. von Euler, J. Berendson, A. Thörne, P. Wersäll, I. Näslund, a. S. Lagerstedt, K. Narfström, and J. M. Olsson, "Electrochemical treatment of tumours." *Bioelectrochemistry*, vol. 51, no. 1, pp. 1–11, feb 2000.

[30] L. E. B. Cabrales, J. J. G. Nava, A. R. Aguilera, J. a. G. Joa, H. M. C. Ciria, M. M. González, M. F. Salas, M. V. Jarque, T. R. González, M. a. O. Mateus, S. C. A. Brooks, F. S. Palencia, L. O. Zamora, M. C. C. Quevedo, S. E. Seringe, V. C. Cuitié, I. B. Cabrales, and G. S. González, "Modified Gompertz equation for electrotherapy murine tumor growth kinetics: predictions and new hypotheses." *BMC cancer*, vol. 10, no. 1, p. 589, jan 2010.

[31] T. Tsong, "Electroporation of cell membranes," *Biophysical Journal*, vol. 60, no. 2, pp. 297–306, 1991.

[32] A. Ivorra and B. Rubinsky, "Historical Review of Irreversible Electroporation in Medicine," in *Irreversible Electroporation*, ser. Series in Biomedical Engineering, B. Rubinsky, Ed. Berlin, Heidelberg: Springer Berlin Heidelberg, 2010, pp. 1–21.

[33] Y. Granot and B. Rubinsky, "Mass transfer model for drug delivery in tissue cells with reversible electroporation," *International Journal of Heat and Mass Transfer*, vol. 51, no. 23-24, pp. 5610–5616, nov 2008.

[34] L. Mir, S. Orlowski, J. Belehradek, and C. Paoletti, "Electrochemotherapy potentiation of antitumour effect of bleomycin by local electric pulses." *European Journal of Cancer*, vol. 27, no. 1, pp. 68–72, 1991.

[35] R. R. Davalos and B. Rubinsky, "Tissue ablation with irreversible electroporation," p. 29, 2004.

[36] E. Maor, A. Ivorra, J. Leor, and B. Rubinsky, "The effect of irreversible electroporation on blood vessels." *Technology in cancer research & treatment*, vol. 6, no. 4, pp. 307–312, 2007.

[37] B. Mali, T. Jarm, M. Snoj, G. Sersa, and D. Miklavcic, "Antitumor effectiveness of electrochemotherapy: A systematic review and meta-analysis," *European Journal of Surgical Oncology*

(EJSO), vol. 39, no. 1, pp. 4–16, jan 2013.

[38] K.-f. Lee, J. Wong, J. W.-y. Hui, Y.-s. Cheung, C. C.-n. Chong, A. K.-w. Fong, S. C.-h. Yu, and P. B.-s. Lai, "Long-term outcomes of microwave versus radiofrequency ablation for hepatocellular carcinoma by surgical approach: A retrospective comparative study," *Asian Journal of Surgery*, pp. 1–8, feb 2016.

[39] V. De Meijer, C. Verhoef, J. Kuiper, I. Alwayn, G. Kazemier, and J. Ijzermans, "Radiofrequency ablation in patients with primary and secondary hepatic malignancies," *J Gastrointest Surg*, vol. 10, pp. 960–73, 2006.

[40] T. Setoyama, S. Natsugoe, H. Okumura, M. Matsumoto, Y. Uchikado, N. Yokomakura, S. Ishigami, and T. Aikou, "a-Catenin is a significant prognostic factor than E-cadherin in esophogeal squamous cell carcinoma," *Journal of surgical oncology*, vol. 95, no. 3, pp. 148–155, 2007.

[41] T. D. Atwell, G. D. Schmit, S. A. Boorjian, J. Mandrekar, A. N. Kurup, A. J. Weisbrod, G. K. Chow, B. C. Leibovich, M. R. Callstrom, D. E. Patterson, C. M. Lohse, and R. H. Thompson, "Percutaneous ablation of renal masses measuring 3.0 cm and smaller: Comparative local control and complications after radiofrequency ablation and cryoablation," *American Journal of Roentgenology*, vol. 200, no. 2, pp. 461–466, 2013.

[42] F. F. Amersi, A. McElrath-Garza, A. Ahmad, T. Zogakis, D. P. Allegra, R. Krasne, and A. J. Bilchik, "Long-term survival after radiofrequency ablation of complex unresectable liver tumors." *Archives of surgery*, vol. 141, no. 6, pp. 581–588, 2006.

[43] S. L. Wong, P. B. Mangu, M. A. Choti, T. S. Crocenzi, G. D. Dodd, G. S. Dorfman, C. Eng, Y. Fong, A. F. Giusti, D. Lu, T. A. Marsland, R. Michelson, G. J. Poston, D. Schrag, J. Seidenfeld, and A. B. Benson, "American Society of Clinical Oncology 2009 clinical evidence review on radiofrequency ablation of hepatic metastases from colorectal cancer," *Journal of Clinical Oncology*, vol. 28, no. 3, pp. 493–508, 2010.

[44] E. D. Kirson, Z. Gurvich, R. Schneiderman, E. Dekel, A. Itzhaki, Y. Wasserman, R. Schatzberger, and Y. Palti, "Disruption of Cancer Cell Replication by Alternating Electric Fields Disruption of Cancer Cell Replication by Alternating Electric Fields," *Cancer research*, vol. 64, pp. 3288–3295, 2004.

[45] S. G. Turner, T. Gergel, H. Wu, M. Lacroix, and S. a. Toms, "The effect of field strength on glioblastoma multiforme re-

sponse in patients treated with the NovoTTF™-100A system." *World journal of surgical oncology*, vol. 12, no. 1, p. 162, 2014.

[46] J. P. Fisher, A. G. Mikos, J. D. Bronzino, and D. R. Peterson, *Tissue Engineering: Principles and Practices*. CRC Press, 2017.

[47] F. S. Barnes and B. Greenebaum, *Handbook of Biological Effects of Electromagnetic Fields*. CRC press, 2006.

[48] S. Grimnes, Ø. G. Martinsen, and O. Martinsen, *Bioimpedance and Bioelectricity Basics*. San Diego: Academic Press, 2000.

[49] F. Booth, "Theory of Electrokinetic Effects," *Nature*, vol. 161, no. 4081, pp. 83–86, jan 1948.

[50] L. a. Geddes, "Historical evolution of circuit models for the electrode-electrolyte interface." *Annals of biomedical engineering*, vol. 25, no. 1, pp. 1–14, 1997.

[51] A. Ivorra, "Electrochemical prevention of needle-tract seeding." *Annals of biomedical engineering*, vol. 39, no. 7, pp. 2080–9, jul 2011.

[52] M.-H. Su, V. Srinivasan, A.-h. Ghanem, and W. I. Higuchi, "Quantitative in Vivo Iontophoretic Studies," *Journal of Pharmaceutical Sciences*, vol. 83, no. 1, pp. 12–17, jan 1994.

[53] G. Marshall, "Biomedical Applications of Electrochemistry, Use of Electric Fields in Cancer Therapy," in *Encyclopedia of Applied Electrochemistry*, G. Kreysa, K.-i. Ota, and R. F. Savinell, Eds. New York, NY: Springer New York, 2014, pp. 126–131.

[54] P. A. Tipler and G. Mosca, *Physics for Scientists and Engineers*, ser. Physics for Scientists and Engineers. W. H. Freeman, 2007, no. parts 1-33.

[55] H. A. Pohl, "Dielectrophoresis: The Behavior of Neutral Matter in Nonuniform Electric Fields." *The Quarterly Review of Biology*, vol. 55, no. 1, pp. 68–69, 1978.

[56] H. A. Pohl and I. Hawk, "Separation of Living and Dead Cells by Dielectrophoresis," *Science*, vol. 152, no. 3722, pp. 647–649, apr 1966.

[57] P. Gascoyne, Xiao-Bo Wang, Ying Huang, and F. Becker, "Dielectrophoretic separation of cancer cells from blood," *IEEE Transactions on Industry Applications*, vol. 33, no. 3, pp. 670–678, 1997.

[58] G. H. Markx, P. A. Dyda, and R. Pethig, "Dielectrophoretic separation of bacteria using a conductivity gradient," *Journal*

of Biotechnology, vol. 51, no. 2, pp. 175–180, 1996.

[59] R. W. Y. Habash, R. Bansal, D. Krewski, and H. T. Alhafid, "Thermal Therapy, Part 1: An Introduction to Thermal Therapy," *Critical Reviews^{TM} in Biomedical Engineering*, vol. 34, no. 6, pp. 459–489, 2006.

[60] C. Gabriel, S. Gabriel, E. H. Grant, E. H. Grant, B. S. J. Halstead, and D. Michael P. Mingos, "Dielectric parameters relevant to microwave dielectric heating," *Chemical Society Reviews*, vol. 27, no. 3, p. 213, 1998.

[61] C. J. Simon, D. E. Dupuy, and W. W. Mayo-Smith, "Microwave ablation: principles and applications." *Radiographics*, vol. 25 Suppl 1, pp. S69–83, 2005.

[62] T. Gutberlet and J. Katsaras, *Lipid Bilayers: Structure and Interactions*, ser. Biological and Medical Physics, Biomedical Engineering. Springer, 2001.

[63] J. F. Ashmore and R. W. Meech, "Ionic basis of membrane potential in outer hair cells of guinea pig cochlea," *Nature*, vol. 322, no. 6077, pp. 368–371, jul 1986.

[64] J. Platkiewicz and R. Brette, "A threshold equation for action potential initiation," *PLoS Computational Biology*, vol. 6, no. 7, p. 25, 2010.

[65] K. W. Horch and G. S. Dhillon, *Neuroprosthetics: Theory and Practice*, ser. Series on bioengineering and biomedical engineering. World Scientific, 2004.

[66] A. Ivorra, "Tissue Electroporation as a Bioelectric Phenomenon: Basic Concepts," in *Irreversible Electroporation*, ser. Series in Biomedical Engineering, B. Rubinsky, Ed. Berlin, Heidelberg: Springer Berlin Heidelberg, 2010, pp. 23–61.

[67] E. Neumann, M. Schaefer-Ridder, Y. Wang, and P. H. Hofschneider, "Gene transfer into mouse lyoma cells by electroporation in high electric fields." *The EMBO journal*, vol. 1, no. 7, pp. 841–5, 1982.

[68] J. C. Weaver and Y. A. Chizmadzhev, "Theory of electroporation: A review," *Bioelectrochemistry and Bioenergetics*, vol. 41, no. 2, pp. 135–160, dec 1996.

[69] A. M. Davies, U. Weinberg, and Y. Palti, "Tumor treating fields: a new frontier in cancer therapy." *Annals of the New York Academy of Sciences*, vol. 1291, no. 1, pp. 86–95, jul 2013.

[70] E. D. Kirson, V. Dbalý, F. Tovarys, J. Vymazal, J. F. Soustiel, A. Itzhaki, D. Mordechovich, S. Steinberg-Shapira, Z. Gur-

vich, R. Schneiderman, Y. Wasserman, M. Salzberg, B. Ryffel, D. Goldsher, E. Dekel, and Y. Palti, "Alternating electric fields arrest cell proliferation in animal tumor models and human brain tumors." *Proceedings of the National Academy of Sciences of the United States of America*, vol. 104, no. 24, pp. 10 152–7, jun 2007.

[71] FDA, "US Food and Drug Administration: NovoTTF-100A System - P100034." Food and Drug Administration, Tech. Rep., 2011.

[72] E. D. Kirson, R. S. Schneiderman, V. Dbalý, F. Tovarys, J. Vymazal, A. Itzhaki, D. Mordechovich, Z. Gurvich, E. Shmueli, D. Goldsher, Y. Wasserman, and Y. Palti, "Chemotherapeutic treatment efficacy and sensitivity are increased by adjuvant alternating electric fields (TTFields)." *BMC medical physics*, vol. 9, p. 1, jan 2009.

[73] R. Stupp, A. Kanner, H. Engelhard, V. Heidecke, S. Taillibert, F. Lieberman, V. Dbaly, E. D. Kirson, Y. Palti, and P. H. Gutin, "A prospective, randomized, open label, phase III clinical trial of NovoTTF-100A vs best standard of care chemotherapy in patients with recurrent glioblastoma," *NeuroOncology*, vol. 12, p. iii3, 2010.

[74] A. V. Titomirov, S. Sukharev, and E. Kistanova, "In vivo electroporation and stable transformation of skin cells of newborn mice by plasmid DNA." *Biochimica et Biophysica Acta*, vol. 1088, no. 1, pp. 131–134, 1991.

[75] E. Neumann, "Membrane electroporation and direct gene transfer," *Bioelectrochemistry and Bioenergetics*, vol. 28, no. 1-2, pp. 247–267, 1992.

[76] J. A. Nickoloff, *Electroporation Protocols for Microorganisms.* Totowa: Humana Press, 1995.

[77] A. Rieder, T. Schwartz, K. Schön-Hölz, S. M. Marten, J. Süß, C. Gusbeth, W. Kohnen, W. Swoboda, U. Obst, and W. Frey, "Molecular monitoring of inactivation efficiencies of bacteria during pulsed electric field treatment of clinical wastewater," *Journal of Applied Microbiology*, vol. 105, no. 6, pp. 2035–2045, 2008.

[78] M. Belehradek, C. Domenge, B. Luboinski, S. Orlowski, J. J. Belehradek, and L. M. Mir, "Electrochemotherapy, a new antitumor treatment. First clinical phase I-II trial." *Cancer*, vol. 72, no. 12, pp. 694–700, 1993.

[79] L. C. Heller and R. Heller, "In vivo electroporation for gene therapy." *Human gene therapy*, vol. 17, no. 9, pp. 890–7, sep 2006.

[80] A. Županič, S. Čorović, and D. Miklavčič, "Optimization of electrode position and electric pulse amplitude in electrochemotherapy," *Radiology and Oncology*, vol. 42, no. 2, pp. 93–101, jan 2008.

[81] A. Golberg and M. L. Yarmush, "Nonthermal irreversible electroporation: fundamentals, applications, and challenges." *IEEE transactions on bio-medical engineering*, vol. 60, no. 3, pp. 707–14, mar 2013.

[82] G. Sersa, "The state-of-the-art of electrochemotherapy before the ESOPE study; advantages and clinical uses," *European Journal of Cancer Supplements*, vol. 4, no. 11, pp. 52–59, nov 2006.

[83] M. Marty, G. Sersa, J. R. Garbay, J. Gehl, C. G. Collins, M. Snoj, V. Billard, P. F. Geertsen, J. O. Larkin, D. Miklavcic, I. Pavlovic, S. M. Paulin-Kosir, M. Cemazar, N. Morsli, D. M. Soden, Z. Rudolf, C. Robert, G. C. O'Sullivan, and L. M. Mir, "Electrochemotherapy – An easy, highly effective and safe treatment of cutaneous and subcutaneous metastases: Results of ESOPE (European Standard Operating Procedures of Electrochemotherapy) study," *European Journal of Cancer Supplements*, vol. 4, no. 11, pp. 3–13, nov 2006.

[84] D. Miklavčič, G. Serša, E. Brecelj, J. Gehl, D. Soden, G. Bianchi, P. Ruggieri, C. R. Rossi, L. G. Campana, and T. Jarm, "Electrochemotherapy: technological advancements for efficient electroporation-based treatment of internal tumors." *Medical & biological engineering & computing*, vol. 50, no. 12, pp. 1213–25, dec 2012.

[85] J. Gehl and K. Videbaek, "Electrode introducer device," 2009.

[86] Y. Guo, Y. Zhang, R. Klein, G. M. Nijm, A. V. Sahakian, R. A. Omary, G.-Y. Yang, and A. C. Larson, "Irreversible electroporation therapy in the liver: longitudinal efficacy studies in a rat model of hepatocellular carcinoma." *Cancer Research*, vol. 70, no. 4, pp. 1555–1563, 2010.

[87] A. José, L. Sobrevals, A. Ivorra, and C. Fillat, "Irreversible electroporation shows efficacy against pancreatic carcinoma without systemic toxicity in mouse models." *Cancer letters*, vol. 317, no. 1, pp. 16–23, apr 2012.

[88] R. E. Neal, J. H. Rossmeisl, J. L. Robertson, C. B. Arena, E. M. Davis, R. N. Singh, J. Stallings, and R. V. Davalos, "Improved Local and Systemic Anti-Tumor Efficacy for Irreversible Electroporation in Immunocompetent versus Immunodeficient Mice," *PLoS One*, vol. 8, no. 5, p. e64559, may 2013.

[89] J. Gehl, T. Skovsgaard, and L. M. Mir, "Vascular reactions to in vivo electroporation: characterization and consequences for drug and gene delivery." *Biochimica et biophysica acta*, vol. 1569, no. 1-3, pp. 51–8, jan 2002.

[90] G. Onik and B. Rubinsky, "Irreversible Electroporation : First Patient Experience Focal Therapy of Prostate Cancer," *Irreversible electroporation*, no. 6, pp. 235–247, 2010.

[91] J. J. Wendler, M. Pech, S. Blaschke, M. Porsch, A. Janitzky, M. Ulrich, O. Dudeck, J. Ricke, and U.-B. Liehr, "Angiography in the isolated perfused kidney: radiological evaluation of vascular protection in tissue ablation by nonthermal irreversible electroporation." *Cardiovascular and interventional radiology*, vol. 35, no. 2, pp. 383–90, 2012.

[92] T. P. Kingham, A. M. Karkar, M. I. D'Angelica, P. J. Allen, R. P. Dematteo, G. I. Getrajdman, C. T. Sofocleous, S. B. Solomon, W. R. Jarnagin, and Y. Fong, "Ablation of perivascular hepatic malignant tumors with irreversible electroporation." pp. 379–87, 2012.

[93] R. C. G. Martin, K. McFarland, S. Ellis, and V. Velanovich, "Irreversible Electroporation in Locally Advanced Pancreatic Cancer: Potential Improved Overall Survival," *Annals of Surgical Oncology*, vol. 20, no. S3, pp. 443–449, dec 2013.

[94] R. C. Martin, K. McFarland, S. Ellis, and V. Velanovich, "Irreversible Electroporation Therapy in the Management of Locally Advanced Pancreatic Adenocarcinoma," *Journal of the American College of Surgeons*, vol. 215, no. 3, pp. 361–369, sep 2012.

[95] A. Deodhar, T. Dickfeld, G. W. Single, W. C. Hamilton, R. H. Thornton, C. T. Sofocleous, M. Maybody, M. Gónen, B. Rubinsky, and S. B. Solomon, "Irreversible electroporation near the heart: ventricular arrhythmias can be prevented with ECG synchronization." *AJR. American journal of roentgenology*, vol. 196, no. 3, pp. W330–5, mar 2011.

[96] S. Bagla and D. Papadouris, "Percutaneous irreversible electroporation of surgically unresectable pancreatic cancer: a case report." *Journal of Vascular and Interventional Radiology (SIR)*,

vol. 23, no. 1, pp. 142–5, 2012.

[97] J. Bruix, F. Izzo, L. Crocetti, V. Vilgrain, M. Abdel-Rehim, L. Bianchi, J. Ricke, M. Pech, and R. Lencioni, "Irreversible Electroporation for the treatment of early-stage hepatocellular carcinoma. A prospective multicenter phase 2 study assessing safety and efficacy," *Journal of Hepatology*, vol. 56, no. 2, p. S554, apr 2012.

[98] B. Rubinsky, G. Onik, and P. Mikus, "Irreversible electroporation: a new ablation modality - clinical implications." *Technology in cancer research & treatment*, vol. 6, no. 1, pp. 37–48, feb 2007.

[99] L. H. Ramirez, S. Orlowski, D. An, G. Bindoula, R. Dzodic, P. Ardouin, C. Bognel, J. Belehradek, J. N. Munck, and L. M. Mir, "Electrochemotherapy on liver tumours in rabbits." *British journal of cancer*, vol. 77, no. 12, pp. 2104–11, jun 1998.

[100] G. Sersa, T. Jarm, T. Kotnik, A. Coer, M. Podkrajsek, M. Sentjurc, D. Miklavcic, M. Kadivec, S. Kranjc, A. Secerov, and M. Cemazar, "Vascular disrupting action of electroporation and electrochemotherapy with bleomycin in murine sarcoma." *British journal of cancer*, vol. 98, no. 2, pp. 388–98, jan 2008.

[101] C. B. Arena and R. V. Davalos, "Advances in Therapeutic Electroporation to Mitigate Muscle Contractions," *Journal of Membrane Science & Technology*, vol. 02, no. 01, pp. 2–4, 2012.

[102] B. Mali, T. Jarm, S. Corovic, M. S. Paulin-Kosir, M. Cemazar, G. Sersa, and D. Miklavcic, "The effect of electroporation pulses on functioning of the heart," *Medical & Biological Engineering & Computing*, vol. 46, no. 8, pp. 745–757, 2008.

[103] C. B. Arena, M. B. Sano, M. N. Rylander, and R. V. Davalos, "Theoretical considerations of tissue electroporation with high-frequency bipolar pulses," *IEEE Transactions on Biomedical Engineering*, vol. 58, no. 5, pp. 1474–1482, 2011.

[104] H. Schwant, "Electrical properties of tissue and cell suspension," *Advances in Biological and Medical Physics*, no. 5, pp. 147–209, 1957.

[105] B. Mercadal, P. T. Vernier, and A. Ivorra, "Dependence of Electroporation Detection Threshold on Cell Radius: An Explanation to Observations Non Compatible with Schwan's Equation Model," *Journal of Membrane Biology*, vol. 249, no. 5, pp. 663–676, 2016.

[106] B. Rubinsky, *Irreversible Electroporation*, B. Rubinsky, Ed.

Springer Verlag, 2009.

[107] A. Ivorra, L. M. Mir, and B. Rubinsky, "Electric field redistribution due to conductivity changes during tissue electroporation: Experiments with a simple vegetal model," in *IFMBE Proceedings*, vol. 25/13, no. 13, 2010, pp. 59–62.

[108] D. Cukjati, D. Batiuskaite, F. André, D. Miklavcic, and L. M. Mir, "Real time electroporation control for accurate and safe in vivo non-viral gene therapy." *Bioelectrochemistry*, vol. 70, no. 2, pp. 501–7, may 2007.

[109] M. Hibino, H. Itoh, and K. Kinosita, "Time courses of cell electroporation as revealed by submicrosecond imaging of transmembrane potential," *Biophysical Journal*, vol. 64, no. 6, pp. 1789–1800, jun 1993.

[110] D. Sel, D. Cukjati, D. Batiuskaite, T. Slivnik, L. Mir, and D. Miklavcic, "Sequential Finite Element Model of Tissue Electropermeabilization," *IEEE Transactions on Biomedical Engineering*, vol. 52, no. 5, pp. 816–827, may 2005.

[111] J. Liang, A. W.-k. Mok, Y. Zhu, and J. Shi, "Resonance versus linear responses to alternating electric fields induce mechanistically distinct mammalian cell death," *Bioelectrochemistry*, vol. 94, pp. 61–68, dec 2013.

[112] E. D. Kirson, M. Giladi, Z. Gurvich, A. Itzhaki, D. Mordechovich, R. S. Schneiderman, Y. Wasserman, B. Ryffel, D. Goldsher, and Y. Palti, "Alternating electric fields (TTFields) inhibit metastatic spread of solid tumors to the lungs." *Clinical & experimental metastasis*, vol. 26, no. 7, pp. 633–40, jan 2009.

[113] R. S. Schneiderman, E. Shmueli, E. D. Kirson, and Y. Palti, "TTFields alone and in combination with chemotherapeutic agents effectively reduce the viability of MDR cell sub-lines that over-express ABC transporters." *BMC cancer*, vol. 10, p. 229, jan 2010.

[114] R. Stupp, E. T. Wong, A. a. Kanner, D. Steinberg, H. Engelhard, V. Heidecke, E. D. Kirson, S. Taillibert, F. Liebermann, V. Dbalý, Z. Ram, J. L. Villano, N. Rainov, U. Weinberg, D. Schiff, L. Kunschner, J. Raizer, J. Honnorat, A. Sloan, M. Malkin, J. C. Landolfi, F. Payer, M. Mehdorn, R. J. Weil, S. C. Pannullo, M. Westphal, M. Smrcka, L. Chin, H. Kostron, S. Hofer, J. Bruce, R. Cosgrove, N. Paleologous, Y. Palti, and P. H. Gutin, "NovoTTF-100A versus physician's choice chemotherapy in recurrent glioblastoma: A randomised phase

III trial of a novel treatment modality," *European Journal of Cancer*, vol. 48, no. 14, pp. 2192–2202, sep 2012.

[115] A. Chakravarti, "Quantitatively Determined Survivin Expression Levels Are of Prognostic Value in Human Gliomas," *Journal of Clinical Oncology*, vol. 20, no. 4, pp. 1063–1068, feb 2002.

[116] J. Overgaard, D. Gonzalez Gonzalez, M. C. C. H. Hulshof, G. Arcangeli, O. Dahl, O. Mella, and S. M. Bentzen, "Hyperthermia as an adjuvant to radiation therapy of recurrent or metastatic malignant melanoma. A multicentre randomized trial by the European Society for Hyperthermic Oncology. 1996." *International journal of hyperthermia : the official journal of European Society for Hyperthermic Oncology, North American Hyperthermia Group*, vol. 25, no. 5, pp. 323–34, aug 2009.

[117] X.-J. Yang, C.-Q. Huang, T. Suo, L.-J. Mei, G.-L. Yang, F.-L. Cheng, Y.-F. Zhou, B. Xiong, Y. Yonemura, and Y. Li, "Cytoreductive surgery and hyperthermic intraperitoneal chemotherapy improves survival of patients with peritoneal carcinomatosis from gastric cancer: final results of a phase III randomized clinical trial." *Annals of surgical oncology*, vol. 18, no. 6, pp. 1575–81, jun 2011.

[118] J. van der Zee, "Heating the patient: a promising approach?" *Annals of Oncology*, vol. 13, no. 8, pp. 1173–1184, aug 2002.

[119] E. P. Armour, D. McEachern, Z. Wang, P. M. Corry, and A. Martinez, "Sensitivity of human cells to mild hyperthermia." *Cancer research*, vol. 53, no. 12, pp. 2740–4, jun 1993.

[120] A. Ivorra and B. Rubinsky, "Electric field modulation in tissue electroporation with electrolytic and non-electrolytic additives." *Bioelectrochemistry*, vol. 70, no. 2, pp. 551–60, may 2007.

[121] A. Ivorra, B. Al-Sakere, B. Rubinsky, and L. M. Mir, "Use of conductive gels for electric field homogenization increases the antitumor efficacy of electroporation therapies." *Physics in medicine and biology*, vol. 53, no. 22, pp. 6605–18, nov 2008.

[122] N. Pavselj, Z. Bregar, D. Cukjati, D. Batiuskaite, L. M. Mir, and D. Miklavčič, "The course of tissue permeabilization studied on a mathematical model of a subcutaneous tumor in small animals." *IEEE transactions on bio-medical engineering*, vol. 52, no. 8, pp. 1373–81, aug 2005.

[123] J. F. Edd, L. Horowitz, R. V. Davalos, L. M. Mir, and B. Rubinsky, "In vivo results of a new focal tissue ablation technique: irreversible electroporation." *IEEE transactions on bio-medical*

engineering, vol. 53, no. 7, pp. 1409–15, jul 2006.

[124] I. Lacković, R. Magjarević, and D. Miklavčič, "Three-dimensional finite-element analysis of joule heating in electrochemotherapy and in vivo gene electrotransfer," *IEEE Transactions on Dielectrics and Electrical Insulation*, vol. 16, no. 5, pp. 1338–1347, oct 2009.

[125] U. Pliquett and R. Nuccitelli, "Measurement and simulation of Joule heating during treatment of B-16 melanoma tumors in mice with nanosecond pulsed electric fields." *Bioelectrochemistry*, pp. 1–7, mar 2014.

[126] H. H. Pennes, "Analysis of tissue and arterial blood temperatures in the resting human forearm. 1948." *Journal of applied physiology*, vol. 85, no. 1, pp. 5–34, jul 1998.

[127] Y.-G. Lv and J. Liu, "A theoretical way of distinguishing the thermal and non-thermal effects in biological tissues subject to EM radiation," *Forschung im Ingenieurwesen*, vol. 67, no. 6, pp. 242–253, apr 2003.

[128] D. a. Nelson and S. a. Nunneley, "Brain temperature and limits on transcranial cooling in humans: quantitative modeling results." *European journal of applied physiology and occupational physiology*, vol. 78, no. 4, pp. 353–9, sep 1998.

[129] C. Gabriel, S. Gabriel, E. Corthout, R. W. Lau, and C. Gabriel, "The Dielectric Properties of biological tissues II. Measurements in the frequency range 10 Hz to 20 GHz," *Physics in medicine and biology*, vol. 41, no. 11, pp. 2251–69, nov 1996.

[130] A. Ibrahiem, C. Dale, W. Tabbara, and J. Wiart, "Analysis of the Temperature Increase Linked to the Power Induced by RF Source," *Progress In Electromagnetics Research*, vol. 52, pp. 23–46, 2005.

[131] J. Lang, B. Erdmann, and M. Seebass, "Impact of nonlinear heat transfer on temperature control in regional hyperthermia." *IEEE transactions on bio-medical engineering*, vol. 46, no. 9, pp. 1129–38, sep 1999.

[132] S. Laufer, A. Ivorra, V. E. Reuter, B. Rubinsky, and S. B. Solomon, "Electrical impedance characterization of normal and cancerous human hepatic tissue." *Physiological measurement*, vol. 31, no. 7, pp. 995–1009, jul 2010.

[133] S. M. Becker and a. V. Kuznetsov, "Local temperature rises influence in vivo electroporation pore development: a numerical stratum corneum lipid phase transition model." *Journal of*

biomechanical engineering, vol. 129, no. 5, pp. 712–21, oct 2007.

[134] J. Brandup, E. Immergut, and E. Grulke, *Polymer handbook*. John Wiley & Sons, Inc., 1999.

[135] M. Gad-el Hak and W. Seemann, "MEMS Handbook," *Applied Mechanics Reviews*, vol. 55, no. 6, p. B109, 2002.

[136] E. J. Berjano, F. Burdío, A. C. Navarro, J. M. Burdío, A. Güemes, O. Aldana, P. Ros, R. Sousa, R. Lozano, E. Tejero, M. A. de Gregorio, and M. a. D. Gregorio, "Improved perfusion system for bipolar radiofrequency ablation of liver: preliminary findings from a computer modeling study," *Physiological Measurement*, vol. 27, no. 10, pp. N55–N66, 2006.

[137] A. Kholodenko, V. Riadovikov, and H. Moser, "The Thermal and Mechanical Properties of Glues for the Atlas SCT Module Assembly," *CERN-ATL-INDET*, vol. 007, 2000.

[138] M. Vives, M. M. Ginestà, K. Gracova, M. Graupera, O. Casanovas, G. Capellà, T. Serrano, B. Laquente, and F. Viñals, "Metronomic chemotherapy following the maximum tolerated dose is an effective anti-tumour therapy affecting angiogenesis, tumour dissemination and cancer stem cells," *International Journal of Cancer*, vol. 133, no. 10, pp. 2464–2472, nov 2013.

[139] M. M. Tomayko and C. P. Reynolds, "Determination of subcutaneous tumor size in athymic (nude) mice," *Cancer Chemotherapy and Pharmacology*, vol. 24, no. 3, pp. 148–154, sep 1989.

[140] B. Laquente, C. Lacasa, M. M. Ginestà, O. Casanovas, A. Figueras, M. Galán, I. G. Ribas, J. R. Germà, G. Capellà, and F. Viñals, "Antiangiogenic effect of gemcitabine following metronomic administration in a pancreas cancer model." *Molecular cancer therapeutics*, vol. 7, no. 3, pp. 638–47, mar 2008.

[141] J. Morren, B. Roodenburg, and S. W. de Haan, "Electrochemical reactions and electrode corrosion in pulsed electric field (PEF) treatment chambers," *Innovative Food Science & Emerging Technologies*, vol. 4, no. 3, pp. 285–295, sep 2003.

[142] N. Mahrour, R. Pologea-Moraru, M. G. Moisescu, S. Orlowski, P. Levêque, and L. M. Mir, "In vitro increase of the fluid-phase endocytosis induced by pulsed radiofrequency electromagnetic fields: importance of the electric field component." *Biochimica et biophysica acta*, vol. 1668, no. 1, pp. 126–37, feb 2005.

[143] L. M. Bareford and P. W. Swaan, "Endocytic mechanisms for targeted drug delivery." *Advanced drug delivery reviews*, vol. 59,

no. 8, pp. 748–58, aug 2007.

[144] J. Busquets, J. Fabregat, R. Jorba, F. G. Borobia, C. Valls, T. Serrano, J. Torras, and L. Lladó, "Indications and results of pancreatic surgery preserving the duodenopancreatic region," *Cirugia espanola*, vol. 82, no. 2, pp. 105–111, 2007.

[145] E. Neumann, A. E. Sowers, and C. A. Jordan, Eds., *Electroporation and Electrofusion in Cell Biology.* Boston, MA: Springer US, 1989.

[146] B. Al-Sakere, F. André, C. Bernat, E. Connault, P. Opolon, R. V. Davalos, B. Rubinsky, and L. M. Mir, "Tumor Ablation with Irreversible Electroporation," *PLoS One*, vol. 2, no. 11, p. e1135, nov 2007.

[147] H. Potter and R. Heller, "Transfection by Electroporation," in *Current Protocols in Molecular Biology.* Hoboken, NJ, USA: John Wiley & Sons, Inc., may 2003, no. 813.

[148] J. González-Sosa, A. Ruiz-Vargas, G. Arias, and A. Ivorra, "Fast flow-through non-thermal pasteurization using constant radiofrequency electric fields," *Innovative Food Science and Emerging Technologies*, vol. 22, pp. 116–123, 2014.

[149] J. Raso, M. L. Calderón, M. Góngora, G. V. Barbosa-Cánovas, and B. G. Swanson, "Inactivation of Zygosaccharomyces Bailii in Fruit Juices by Heat, High Hydrostatic Pressure and Pulsed Electric Fields," *Journal of Food Science*, vol. 63, no. 6, pp. 1042–1044, 2006.

[150] M. Takahashi, T. Furukawa, H. Saitoh, A. Aoki, T. Koike, Y. Moriyama, and A. Shibata, "Gene Transfer into Human Leukemia Cell Lines by Electroporation: Experience with Exponentially Decaying and Sqaure Wave Pulse," *Leukemia Research*, vol. 15, no. 6, pp. 507–13, 1991.

[151] M. Kandušer, D. Miklavčič, and M. Pavlin, "Mechanisms involved in gene electrotransfer using high- and low-voltage pulses - An in vitro study," *Bioelectrochemistry*, vol. 74, no. 2, pp. 265–271, 2009.

[152] L. C. Heller and R. Heller, "In Vivo Electroporation for Gene Therapy," *Human Gene Therapy*, vol. 17, no. 9, pp. 890–897, sep 2006.

[153] C. B. Arena, M. B. Sano, J. H. Rossmeisl, J. L. Caldwell, P. a. Garcia, M. N. Rylander, and R. V. Davalos, "High-frequency irreversible electroporation (H-FIRE) for non-thermal ablation without muscle contraction." *Biomedical engineering online*,

vol. 10, no. 1, p. 102, jan 2011.

[154] M. Breton and L. M. Mir, "Microsecond and nanosecond electric pulses in cancer treatments," *Bioelectromagnetics*, vol. 33, no. 2, pp. 106–123, 2012.

[155] R. Nuccitelli, U. Pliquett, X. Chen, W. Ford, R. James Swanson, S. J. Beebe, J. F. Kolb, and K. H. Schoenbach, "Nanosecond pulsed electric fields cause melanomas to self-destruct," *Biochemical and Biophysical Research Communications*, vol. 343, no. 2, pp. 351–360, 2006.

[156] M. Rebersek and D. Miklavčič, "Concepts of Electroporation Pulse Generation and Overview of Electric Pulse Generators for Cell and Tissue Electroporation," in *Advanced Electroporation Techniques in Biology and Medicine*, A. G. Pakhomov, D. Miklavčič, and M. S. Markov, Eds. CRC Press, 2010, pp. 323 –339.

[157] M. Reberšek, D. Miklavčič, C. Bertacchini, and M. Sack, "Cell membrane electroporation-Part 3: The equipment," *IEEE Electrical Insulation Magazine*, vol. 30, no. 3, pp. 8–18, 2014.

[158] J. S. Glaser, J. J. Nasadoski, P. A. Losee, A. S. Kashyap, K. S. Matocha, J. L. Garrett, and L. D. Stevanovic, "Direct comparison of silicon and silicon carbide power transistors in high-frequency hard-switched applications," *Conference Proceedings - IEEE Applied Power Electronics Conference and Exposition - APEC*, pp. 1049–1056, 2011.

[159] A. G. Pakhomov, D. Miklavcic, and M. S. Markov, *Advanced Electroporation Techniques in Biology and Medicine*. CRC Press, 2010.

[160] M. Puc, S. Corović, K. Flisar, M. Petkovsek, J. Nastran, and D. Miklavcic, "Techniques of signal generation required for electropermeabilization. Survey of electropermeabilization devices." *Bioelectrochemistry*, vol. 64, no. 2, pp. 113–24, sep 2004.

[161] M. Petkovsek, J. Nastran, D. Voncina, P. Zajec, D. Miklavcic, and G. Sersa, "High voltage pulse generation," *Electronics Letters*, vol. 38, no. 14, p. 680, 2002.

[162] C. Suárez, A. Soba, F. Maglietti, N. Olaiz, and G. Marshall, "The Role of Additional Pulses in Electropermeabilization Protocols," *PLoS One*, vol. 9, no. 12, p. e113413, 2014.

[163] I. Ashie and B. Simpson, "Application of high hydrostatic pressure to control enzyme related fresh seafood texture deterioration," pp. 569–575, 1996.

[164] R. N. Pereira, F. G. Galindo, A. A. Vicente, and P. Dejmek, "Effects of pulsed electric field on the viscoelastic properties of potato tissue," *Food Biophysics*, vol. 4, no. 3, pp. 229–239, 2009.

[165] A. A. Elserougi, A. M. Massoud, and S. Ahmed, "A Modular High-Voltage Pulse-Generator with Sequential Charging for Water Treatment Applications," *IEEE Transactions on Industrial Electronics*, vol. 63, no. 12, pp. 7898–7907, 2016.

[166] L. Redondo, J. F. Silva, and E. Margato, "Modular pulsed generator for kV and kHz applications based on forward converters association," in *2007 European Conference on Power Electronics and Applications*. IEEE, 2007, pp. 1–7.

[167] S.-b. Ok, H.-j. Ryoo, S.-r. Jang, S.-h. Ahn, and G. Goussev, "Design of a High-Efficiency 40-kV, 150-A, 3-kHz Solid-State Pulsed Power Modulator," *IEEE Transactions on Plasma Science*, vol. 40, no. 10, pp. 2569–2577, oct 2012.

[168] J. F. Egan and D. A. Mortensen, "A comparison of land-sharing and land-sparing strategies for plant richness conservation in agricultural landscapes," *Ecological Applications*, vol. 22, no. 2, pp. 459–471, mar 2012.

[169] N. Otsu, "A Threshold Selection Method from Gray-Level Histograms," *IEEE Transactions on Systems, Man, and Cybernetics*, vol. 9, no. 1, pp. 62–66, jan 1979.

[170] R. Pérez-Delgado, G. Velasco-Quesada, and M. Román-Lumbreras, "Current sharing control strategy for IGBTs connected in parallel," *Journal of Power Electronics*, vol. 16, no. 2, pp. 769–777, 2016.

[171] R. Qasrawi, L. Silve, F. Burdío, Z. Abdeen, and A. Ivorra, "Anatomically Realistic Simulations of Liver Ablation by Irreversible Electroporation," *Technology in Cancer Research & Treatment*, p. 153303461668747, 2017.

[172] G. Pucihar, J. Krmelj, M. Reberšek, T. B. Napotnik, and D. Miklavčič, "Equivalent pulse parameters for electroporation," *IEEE Transactions on Biomedical Engineering*, vol. 58, no. 11, pp. 3279–3288, 2011.

[173] C. V. Greenway and R. D. Stark, "Hepatic vascular bed." *Physiological reviews*, vol. 51, no. 1, pp. 23–65, jan 1971.

[174] C. V. Greenway and W. W. Lautt, "Hepatic circulation," in *Comprehensive Physiology*. Hoboken, NJ, USA: John Wiley & Sons, Inc., jan 2011, pp. 1519–64.

[175] A. Ananthakrishnan, V. Gogineni, and K. Saeian, "Epidemiol-

ogy of primary and secondary liver cancers." *Seminars in interventional radiology*, vol. 23, no. 1, pp. 47–63, 2006.

[176] R. Lencioni and L. Crocetti, "Radiofrequency Ablation of Liver Cancer," *Techniques in Vascular and Interventional Radiology*, vol. 10, no. 1, pp. 38–46, 2007.

[177] G. P. Kanas, A. Taylor, J. N. Primrose, W. J. Langeberg, M. A. Kelsh, F. S. Mowat, D. D. Alexander, M. A. Choti, and G. Poston, "Survival after liver resection in metastatic colorectal cancer: Review and meta-analysis of prognostic factors," *Clinical Epidemiology*, vol. 4, no. 1, pp. 283–301, 2012.

[178] J. S. Bolton and G. M. Fuhrman, "Survival after resection of multiple bilobar hepatic metastases from colorectal carcinoma." *Annals of surgery*, vol. 231, no. 5, pp. 743–51, may 2000.

[179] Q. Castellví, P. Sánchez-Velázquez, E. Berjano, F. Burdío, and A. Ivorra, "Selective Electroporation of Liver Tumor Nodules by Means of Hypersaline Infusion: A Feasibility Study," in *6th European Conference of the International Federation for Medical and Biological Engineering*, 2015, pp. 821–824.

[180] G. Garcea, T. D. Lloyd, C. Aylott, G. Maddern, and D. P. Berry, "The emergent role of focal liver ablation techniques in the treatment of primary and secondary liver tumours," *European Journal of Cancer*, vol. 39, no. 15, pp. 2150–2164, 2003.

[181] W. Y. Lau, T. W. T. Leung, S. C. H. Yu, and S. K. W. Ho, "Percutaneous local ablative therapy for hepatocellular carcinoma: a review and look into the future." *Annals of surgery*, vol. 237, no. 2, pp. 171–179, 2003.

[182] M. a. Phillips, R. Narayan, T. Padath, and B. Rubinsky, "Irreversible electroporation on the small intestine." *British journal of cancer*, vol. 106, no. 3, pp. 490–5, 2012.

[183] H. J. Scheffer, K. Nielsen, M. C. De Jong, A. A. J. M. Van Tilborg, J. M. Vieveen, A. Bouwman, S. Meijer, C. Van Kuijk, P. Van Den Tol, and M. R. Meijerink, "Irreversible electroporation for nonthermal tumor ablation in the clinical setting: A systematic review of safety and efficacy," *Journal of Vascular and Interventional Radiology*, vol. 25, no. 7, pp. 997–1011, 2014.

[184] A. Kitao, Y. Zen, O. Matsui, T. Gabata, and Y. Nakanuma, "Hepatocarcinogenesis: multistep changes of drainage vessels at CT during arterial portography and hepatic arteriography–radiologic-pathologic correlation." *Radiology*, vol. 252, no. 2, pp. 605–14, aug 2009.

[185] D. Haemmerich, S. T. Staelin, J. Z. Tsai, S. Tungjitkusolmun, D. M. Mahvi, and J. G. Webster, "In vivo electrical conductivity of hepatic tumours." *Physiological measurement*, vol. 24, no. 2, pp. 251–60, may 2003.

[186] M. K. Kapanen, J. T. Halavaara, and A. M. Häkkinen, "Open four-compartment model in the measurement of liver perfusion," *Academic Radiology*, vol. 12, no. 8, pp. 1542–1550, 2005.

[187] M. Kretowski, J. Bezy-Wendling, and P. Coupe, "Simulation of biphasic CT findings in hepatic cellular carcinoma by a two-level physiological model," *IEEE Transactions on Biomedical Engineering*, vol. 54, no. 3, pp. 538–542, 2007.

[188] L. O. Schwen, A. Schenk, C. Kreutz, J. Timmer, M. M. Bartolomé Rodríguez, L. Kuepfer, and T. Preusser, "Representative Sinusoids for Hepatic Four-Scale Pharmacokinetics Simulations," *PLoS One*, vol. 10, no. 7, p. e0133653, jul 2015.

[189] J. Lu, M. R. Goldsmith, C. M. Grulke, D. T. Chang, R. D. Brooks, J. A. Leonard, M. B. Phillips, E. D. Hypes, M. J. Fair, R. Tornero-Velez, J. Johnson, C. C. Dary, and Y. M. Tan, "Developing a Physiologically-Based Pharmacokinetic Model Knowledgebase in Support of Provisional Model Construction," *PLoS Computational Biology*, vol. 12, no. 2, pp. 1–22, 2016.

[190] W. H. Bickell, S. P. Bruttig, G. A. Millnamow, J. O'Benar, and C. E. Wade, "Use of hypertonic saline/dextran versus lactated ringer's solution as a resuscitation fluid after uncontrolled aortic hemorrhage in anesthetized swine," *Annals of Emergency Medicine*, vol. 21, no. 9, pp. 1077–1085, 1992.

[191] M. C. Mazzoni, P. Borgström, K. E. Arfors, and M. Intaglietta, "Dynamic fluid redistribution in hyperosmotic resuscitation of hypovolemic hemorrhage." *The American journal of physiology*, vol. 255, no. 3 Pt 2, pp. H629–37, sep 1988.

[192] K. Fosters and H. Schwan, "Dielectric properties of tissues," in *Handbook of Biological Effects of Electromagnetic Fields*, C. Polk and E. Postow, Eds. CRC press, 1996, ch. 1, pp. 25–102.

[193] E. D. Trautman and R. S. Newbower, "A practical analysis of the electrical conductivity of blood." *IEEE Transactions on Biomedical Engineeringmedical engineering*, vol. 30, no. 3, pp. 141–54, mar 1983.

[194] S. a. Solazzo, Z. Liu, S. M. Lobo, M. Ahmed, A. U. Hines-Peralta, R. E. Lenkinski, and S. N. Goldberg, "Radiofre-

quency ablation: importance of background tissue electrical conductivity–an agar phantom and computer modeling study." *Radiology*, vol. 236, pp. 495–502, 2005.

[195] M. J. Peters, J. G. Stinstra, I. Leveles, and B. He, "The Electrical Conductivity of Living Tissue: A Parameter in the Bioelectrical Inverse Problem," *Modeling and Imaging of Bioelectrical Activity*, vol. c, no. 1967, pp. 281–319, 2005.

[196] G. Archie, "The Electrical Resistivity Log as an Aid in Determining Some Reservoir Characteristics," *Petroleum Technology*, no. October, pp. 54–62, 1942.

[197] P. W. J. Glover, "A generalized Archie's law for n phases," *Geophysics*, vol. 75, no. 6, p. E247, 2010.

[198] J. Wambaugh and I. Shah, "Simulating Microdosimetry in a Virtual Hepatic Lobule," *PLoS Computational Biology*, vol. 6, no. 4, p. e1000756, 2010.

[199] L. O. Schwen, M. Krauss, C. Niederalt, F. Gremse, F. Kiessling, A. Schenk, T. Preusser, and L. Kuepfer, "Spatio-Temporal Simulation of First Pass Drug Perfusion in the Liver," *PLoS Computational Biology*, vol. 10, no. 3, p. e1003499, mar 2014.

[200] C. V. Greenway, R. D. Stark, and W. W. Lautt, "Capacitance Responses and Fluid Exchange in the Cat Liver during Stimulation of the Hepatic Nerves," *Circulation Research*, vol. 25, no. 3, pp. 277–284, 1969.

[201] P. Garcia-Canadilla, P. a. Rudenick, F. Crispi, M. Cruz-Lemini, G. Palau, O. Camara, E. Gratacos, and B. H. Bijens, "A Computational Model of the Fetal Circulation to Quantify Blood Redistribution in Intrauterine Growth Restriction," *PLoS Computational Biology*, vol. 10, no. 6, pp. 9–11, 2014.

[202] M. Eliakim, S. Z. Rosenberg, and K. Braun, "Effect of Hypertonic Saline on the Pulmonary and Systemic Pressures," *Circulation Research*, vol. 6, no. 3, pp. 357–362, may 1958.

[203] H. J. Semler, J. T. Shepherd, and H. J. Swan, "Pressor effect of hypertonic saline on pulmonary circulation." *Circulation research*, vol. 7, no. November 1959, pp. 1011–1017, 1959.

[204] H. Schmid-Schönbein, R. Wells, and J. Goldstone, "Influence of Deformability of Human Red Cells upon Blood Viscosity," *Circulation Research*, vol. 25, no. 2, pp. 131–143, aug 1969.

[205] S. Keiding, S. Johansen, K. Winkler, K. Tonnesen, and N. Tygstrup, "Michaelis-Menten kinetics of galactose elimination by the isolated perfused pig liver." *The American journal*

of physiology, vol. 230, no. 5, pp. 1302–1313, 1976.

[206] J. H. Siggers, K. Leungchavaphongse, C. H. Ho, and R. Repetto, "Mathematical model of blood and interstitial flow and lymph production in the liver," *Biomechanics and Modeling in Mechanobiology*, vol. 13, no. 2, pp. 363–378, apr 2014.

[207] A. R. Pries, D. Neuhaus, and P. Gaehtgens, "Blood viscosity in tube flow: dependence on diameter and hematocrit." *The American journal of physiology*, vol. 263, no. 6 Pt 2, pp. H1770–H1778, 1992.

[208] A. Blouin, R. P. Bolender, and E. R. Weibel, "Distribution of organelles and membranes between hepatocytes and nonhepatocytes in the rat liver parenchyma. A stereological study." *The Journal of cell biology*, vol. 72, no. 2, pp. 441–55, feb 1977.

[209] S. M. Niehues, J. K. Unger, M. Malinowski, J. Neymeyer, B. Hamm, and M. Stockmann, "Liver volume measurement: reason of the difference between in vivo CT-volumetry and intraoperative ex vivo determination and how to cope it." *European journal of medical research*, vol. 15, pp. 345–350, 2010.

[210] E. Muirhead, R. W. Lackey, J. M. Hill, and A. Bunde, "Transient hypotension following rapid intravenous injections of hypertonic solutions." *Am J Physiol.*, vol. 151, no. 2, pp. 516–524, 1947.

[211] H. J. Adrogué and N. E. Madias, "Hypernatremia," *New England Journal of Medicine*, vol. 342, no. 20, pp. 1493–1499, may 2000.

[212] A. Ivorra and B. Rubinsky, "In vivo electrical impedance measurements during and after electroporation of rat liver." *Bioelectrochemistry*, vol. 70, no. 2, pp. 287–95, may 2007.

[213] J. Zhuang and J. F. Kolb, "Time domain dielectric spectroscopy of nanosecond pulsed electric field induced changes in dielectric properties of pig whole blood." *Bioelectrochemistry*, vol. 103, pp. 28–33, 2015.

[214] L. A. Geddes and L. E. Baker, "The specific resistance of biological material—A compendium of data for the biomedical engineer and physiologist," *Medical & Biological Engineering*, vol. 5, no. 3, pp. 271–293, may 1967.

[215] W. W. Lautt and C. V. Greenway, "Hepatic venous compliance and role of liver as a blood reservoir." *The American journal of physiology*, vol. 231, no. 2, pp. 292–295, 1976.

[216] L. Romano, L. Grazioli, L. Bonomo, J. R. Xu, K. M. Chen,

R. Dore, A. Vanzualli, and C. Catalano, "Enhancement and safety of iomeprol-400 and iodixanol-320 in patients undergoing abdominal multidetector CTL Romano," *British Journal of Radiology*, vol. 82, no. 975, pp. 204–211, 2009.

[217] R. Tyagi, K. Donaldson, C. M. Loftus, and J. Jallo, "Hypertonic saline: A clinical review," *Neurosurgical Review*, vol. 30, no. 4, pp. 277–289, 2007.

[218] T. Ajito, K. Suzuki, and S. Iwabuchi, "Effect of intravenous infusion of a 7.2% hypertonic saline solution on serum electrolytes and osmotic pressure in healthy beagles." *The Journal of veterinary medical science*, vol. 61, no. 6, pp. 637–41, jun 1999.

[219] T. S. Tan, K. H. S. Tan, H. P. Ng, and M. W. Loh, "The effects of hypertonic saline solution (7.5%) on coagulation and fibrinolysis: An in vitro assessment using thromboelastography," *Anaesthesia*, vol. 57, no. 7, pp. 644–648, 2002.

[220] J. Rothbarth, M. E. J. Pijl, A. L. Vahrmeijer, H. H. Hartgrink, F. G. J. Tijl, P. J. K. Kuppen, R. A. E. M. Tollenaar, and C. J. H. Van De Velde, "Isolated hepatic perfusion with high-dose melphalan for the treatment of colorectal metastasis confined to the liver," *British Journal of Surgery*, vol. 90, no. 11, pp. 1391–1397, 2003.

[221] Y.-c. Lin, J.-h. Chen, K.-w. Han, and W.-c. Shen, "Ablation of liver tumor by injection of hypertonic saline." *AJR. American journal of roentgenology*, vol. 184, no. 1, pp. 212–9, jan 2005.

[222] C. Debbaut, D. Monbaliu, C. Casteleyn, P. Cornillie, D. Van Loo, B. Masschaele, J. Pirenne, P. Simoens, L. Van Hoorebeke, and P. Segers, "From vascular corrosion cast to electrical analog model for the study of human liver hemodynamics and perfusion," *IEEE Transactions on Biomedical Engineering*, vol. 58, no. 1, pp. 25–35, 2011.

[223] J. E. Hall, *Guyton and Hall Textbook of Medical Physiology*, ser. Guyton Physiology. Saunders, 2010.

[224] A. J. Hansen and M. Nedergaard, "Brain ion homeostasis in cerebral ischemia," *Neurochemical Pathology*, vol. 9, no. 1, pp. 195–209, 1988.

[225] S. C. Howard, D. P. Jones, and C.-H. Pui, "The Tumor Lysis Syndrome," *New England Journal of Medicine*, vol. 364, no. 19, pp. 1844–1854, may 2011.

[226] G. Saulis, S. Satkauskas, and R. Praneviciūte, "Determination of cell electroporation from the release of intracellular potassium

ions." *Analytical biochemistry*, vol. 360, no. 2, pp. 273–81, jan 2007.

[227] J. M. Colet, J. D. Makos, C. R. Malloy, and A. D. Sherry, "Determination of the intracellular sodium concentration in perfused mouse liver by 31P and 23Na magnetic resonance spectroscopy." *Magnetic Resonance in Medicine*, vol. 39, no. 1, pp. 155–159, 1998.

[228] C. Y. Bhatkhande and V. D. Joglekar, "Fatal poisoning by potassium in human and rabbit," *Forensic Science*, vol. 9, no. C, pp. 33–36, 1977.

[229] R. Ness, "Rodents," in *Exotic Animal Formulary*, J. W. Carpenter, Ed. Elsevier Inc., 2005, ch. 8, pp. 375–409.

[230] K. R. Thomson, W. Cheung, S. J. Ellis, D. Federman, H. Kavnoudias, D. Loader-Oliver, S. Roberts, P. Evans, C. Ball, and A. Haydon, "Investigation of the safety of irreversible electroporation in humans." *Journal of vascular and interventional radiology : JVIR*, vol. 22, no. 5, pp. 611–21, may 2011.

[231] P. Philips, D. Hays, and R. C. G. Martin, "Irreversible electroporation ablation (IRE) of unresectable soft tissue tumors: Learning curve evaluation in the first 150 patients treated," *PLoS One*, vol. 8, no. 11, pp. 1–9, 2013.

[232] G. Narayanan, T. Froud, K. Lo, K. J. Barbery, E. Perez-Rojas, and J. Yrizarry, "Pain analysis in patients with hepatocellular carcinoma: Irreversible electroporation versus radiofrequency ablation - Initial observations," *CardioVascular and Interventional Radiology*, vol. 36, no. 1, pp. 176–182, 2013.

[233] M. Silk, T. Wimmer, G. Getrajdman, C. Sofocleous, J. Durack, and S. Solomon, "Safety of irreversible electroporation (IRE) treatment for metastatic disease in humans," *Journal of Vascular and Interventional Radiology*, vol. 24, no. 4, pp. S21–S22, apr 2013.

[234] J. H. Rossmeisl, P. A. Garcia, T. E. Pancotto, J. L. Robertson, N. Henao-Guerrero, R. E. Neal, T. L. Ellis, and R. V. Davalos, "Safety and feasibility of the NanoKnife system for irreversible electroporation ablative treatment of canine spontaneous intracranial gliomas," *Journal of Neurosurgery*, vol. 123, no. 4, pp. 1008–1025, oct 2015.

[235] K. S. Murray, B. Ehdaie, J. Musser, J. Mashni, G. Srimathveeravalli, J. C. Durack, S. B. Solomon, and J. A. Coleman, "Pilot Study to Assess Safety and Clinical Outcomes of Irre-

versible Electroporation for Partial Gland Ablation in Men with Prostate Cancer," *The Journal of Urology*, vol. 196, no. 3, pp. 883–890, sep 2016.

[236] C. Ball, K. R. Thomson, and H. Kavnoudias, "Irreversible electroporation: a new challenge in "out of operating theater" anesthesia." *Anesthesia and analgesia*, vol. 110, no. 5, pp. 1305–9, may 2010.

List of publications

Journal Papers

1. M. Trujillo, **Q. Castellví**, F. Burdío, P. Sánchez-Velazquez, A. Ivorra, A. Andaluz, and E. Berjano, "Can electroporation previous to radiofrequency hepatic ablation enlarge thermal lesion size? A feasibility study based on theoretical modelling and in vivo experiments.," *Int. J. Hyperthermia*, vol. 29, no. 3, pp. 211–8, May 2013.

2. A. Ivorra, L. Becerra-Fajardo, and **Q. Castellví**, "In vivo demonstration of injectable microstimulators based on charge-balanced rectification of epidermically applied currents," *J. Neural Eng.*, vol. 12, no. 6, p. 66010, 2015.

3. **Q. Castellví**, M. M. Ginestá, G. Capellá, and A. Ivorra, "Tumor growth delay by adjuvant alternating electric fields which appears non-thermally mediated," *Bioelectrochemistry*, vol. 105, pp. 16–24, 2015.

4. P. Sánchez-Velázquez, **Q. Castellví**, A. Villanueva, R. Quesada, C. Pañella, M. Cáceres, D. Dorcaratto, A. Andaluz, X. Moll, M. Trujillo, J. M. Burdío, E. Berjano, L. Grande, A. Ivorra, and F. Burdío, "Irreversible electroporation of the liver: is there a safe limit to the ablation volume?," *Sci. Rep.*, vol. 6, no. April, p. 23781, 2016.

5. H. Sarnago, Ó. Lucía, A. Naval, J. M. Burdío, **Q. Castellví**, and A. Ivorra, "A Versatile Multilevel Converter Platform for Cancer Treatment Using Irreversible Electroporation," *IEEE J.*

Emerg. Sel. Top. Power Electron., vol. 4, no. 1, pp. 236–242, 2016.

6. **Q. Castellví**, P. Sánchez-Velázquez, X. Moll, E. Berjano, A. Andaluz, F. Burdío, B. Bijnens and A. Ivorra, "Modeling Liver Electrical Conductivity during Hypertonic Injection," *Int. j. numer. method. biomed. eng.*, pp. 1–23, 2017.

7. P. Sánchez-Velázquez, **Q. Castellví**, A. Villanueva, M. Iglesias, R. Quesada, C. Pañella, M. Cáceres, D. Dorcaratto, A. Andaluz, X. Moll, M. Trujillo, J. M. Burdío, E. Berjano, L. Grande, A. Ivorra, and F. Burdío, "Long-term effectiveness of irreversible electroporation in a murine model of colorectal liver metastasis." *Sci. Rep.*, vol. 7, no. February, p. 44821, 2017.

Conference Papers

1. **Q. Castellví**, P. Sánchez-Velázquez, E. Berjano, F. Burdío, and A. Ivorra, "Selective Electroporation of Liver Tumor Nodules by Means of Hypersaline Infusion: A Feasibility Study," in *6th European Conference of the International Federation for Medical and Biological Engineering*, pp. 821–824, 2015.

2. **Q. Castellví**, J. Banús, and A. Ivorra, "3D Assessment of Irreversible Electroporation Treatments in Vegetal Models," in *1st World Congress on Electroporation and Pulsed Electric Fields in Biology, Medicine and Food & Environmental Technologies*, pp. 294–297, 2016.

3. C. Bernal, Ó. Lucía, H. Sarnago, J. M. Burdío, A. Ivorra, and **Q. Castellví**, "A review of pulse generation topologies for clinical electroporation," *IECON 2015 - 41st Annu. Conf. IEEE Ind. Electron. Soc.*, pp. 625–630, 2016.

Conference Abstracts

1. **Q. Castellví**, M. M. Ginestá, G. Capellá, and A. Ivorra, "In vivo study using Tumor Treatment Fields (TTFs) and prolonged mild hyperthermia as adjuvant methods for cancer treatment," in *Tenth International Bioelectrics Symposium*, 2013.

2. J. González-Sosa, A. Ruiz-Vargas, G. Arias, **Q. Castellví**, and A. Ivorra, "Fast flow-through non-thermal pasteurization using

constant radiofrequency electric fields," in *Tenth International Bioelectrics Symposium*, 2013.

3. **Q. Castellví**, P. Sánchez-Velázquez, A. Villanueva, E. Berjano, F. Burdío, and A. Ivorra, "Sudden Death of Mice after Irreversible Electroporation of a Large Portion of the Liver: Probable Role of Hyperkalemia," in *1st World Congress on Electroporation and Pulsed Electric Fields in Biology, Medicine and Food & Environmental Technologies*, 2016.

Book Chapters

1. **Q. Castellví**, B. Mercadal, and A. Ivorra, "Assessment of Electroporation by Electrical Impedance Methods," in *Handbook of Electroporation*, D. Miklavčič, Ed. Springer International Publishing, pp. 1–20, 2016.

Patents

1. Filing reference P201531870, "Modular High-Voltage Bipolar Pulse Generator for Electroporation Applications." Priority date: 22-12-2015.

2. Filing reference P201231644, "System for preventing bacterial infections in needle trajectories." Priority date: 25-10-2012.

Curriculum Vitae

Quim Castellví was born in Barcelona, Spain, in 1984. He received the B.Sc. degree in electronics engineering from the Universitat Politècnica de Catalunya, Terrassa, Spain, in 2009, and the M.Sc. degree in biomedical engineering from the Universitat de Barcelona, Barcelona, in 2011. He has been a Research Engineer with Universitat Pompeu Fabra, Barcelona, since 2011. His research interests include cancer treatment by means of electrical methods and, in particular, electroporation. Mr. Castellví received a competitive FPU scholarship from the Spanish Ministry of Education to carry on the PhD studies in 2012.